

Argonne National Laboratory

SOME MEASUREMENTS OF PROMPT-NEUTRON
FISSION YIELD ($\bar{\nu}_p$) IN THERMAL-NEUTRON
FISSION OF ^{232}U , ^{238}Pu , ^{241}Pu , ^{241}Am ,
 $^{242\text{m}}\text{Am}$, ^{243}Cm , ^{245}Cm , AND IN
SPONTANEOUS FISSION OF ^{244}Cm

by

A. H. Jaffey and J. L. Lerner

The facilities of Argonne National Laboratory are owned by the United States Government. Under the terms of a contract (W-31-109-Eng-38) between the U. S. Atomic Energy Commission, Argonne Universities Association and The University of Chicago, the University employs the staff and operates the Laboratory in accordance with policies and programs formulated, approved and reviewed by the Association.

MEMBERS OF ARGONNE UNIVERSITIES ASSOCIATION

The University of Arizona
Carnegie-Mellon University
Case Western Reserve University
The University of Chicago
University of Cincinnati
Illinois Institute of Technology
University of Illinois
Indiana University
Iowa State University
The University of Iowa

Kansas State University
The University of Kansas
Loyola University
Marquette University
Michigan State University
The University of Michigan
University of Minnesota
University of Missouri
Northwestern University
University of Notre Dame

The Ohio State University
Ohio University
The Pennsylvania State University
Purdue University
Saint Louis University
Southern Illinois University
University of Texas
Washington University
Wayne State University
The University of Wisconsin

LEGAL NOTICE

This report was prepared as an account of Government sponsored work. Neither the United States, nor the Commission, nor any person acting on behalf of the Commission:

A. Makes any warranty or representation, expressed or implied, with respect to the accuracy, completeness, or usefulness of the information contained in this report, or that the use of any information, apparatus, method, or process disclosed in this report may not infringe privately owned rights; or

B. Assumes any liabilities with respect to the use of, or for damages resulting from the use of any information, apparatus, method, or process disclosed in this report.

As used in the above, "person acting on behalf of the Commission" includes any employee or contractor of the Commission, or employee of such contractor, to the extent that such employee or contractor of the Commission, or employee of such contractor prepares, disseminates, or provides access to, any information pursuant to his employment or contract with the Commission, or his employment with such contractor.

Printed in the United States of America

Available from

Clearinghouse for Federal Scientific and Technical Information
National Bureau of Standards, U. S. Department of Commerce
Springfield, Virginia 22151

Price: Printed Copy \$3.00; Microfiche \$0.65

ARGONNE NATIONAL LABORATORY
9700 South Cass Avenue
Argonne, Illinois 60439

SOME MEASUREMENTS OF PROMPT-NEUTRON
FISSION YIELD ($\bar{\nu}_p$) IN THERMAL-NEUTRON
FISSION OF ^{232}U , ^{238}Pu , ^{241}Pu , ^{241}Am ,
 $^{242\text{m}}\text{Am}$, ^{243}Cm , ^{245}Cm , AND IN
SPONTANEOUS FISSION OF ^{244}Cm

by

A. H. Jaffey and J. L. Lerner

Chemistry Division

November 1969

TABLE OF CONTENTS

	<u>Page</u>
ABSTRACT	9
1. INTRODUCTION	9
2. $\bar{\nu}_p$ -MEASUREMENT METHOD	10
2.1. General.	10
2.2. Calculation of $\bar{\nu}_p$ from Coincidence Measurements	11
2.3. The Relation of ϵ_n -magnitude to $\bar{\nu}_p$ -calculation	13
3. MEASURING APPARATUS.	15
3.1. General.	15
3.2. Constancy of ϵ_n over the Sample	16
3.3. Neutron Detector	18
3.4. Sensitivity of Method.	19
3.5. Ionization Chamber	19
3.6. Effect of α Pileup	19
3.7. Circuitry. Resolution Losses	20
3.8. Coincidence Time	20
3.9. Standard Samples	21
4. CALCULATIONS, CORRECTIONS, AND SYSTEMATIC EFFECTS.	22
4.1. Correction for Accidentals	22
4.2. Correction for Neutron-detector Drift	22
4.3. Averaging	23
4.4. Correction for Other Fissioning Isotopes	24
4.5. Averaging Results Relative to the Three Standards	25
4.6. Correction for a Spontaneously Fissioning Isotope	26
4.7. Effect of Directional Correlation between Fission Fragment and Fission Neutrons	28
4.8. $\bar{\nu}_p$ -values for the Standards	29

TABLE OF CONTENTS

	<u>Page</u>
4.9. Calibration of Relative Neutron-counting-efficiency Variation with Neutron-energy Spectrum.	29
5. MEASUREMENTS	33
6. MEASUREMENTS AND RESULTS.	33
6.1. ^{241}Pu	33
6.2. ^{238}Pu	36
6.3. ^{241}Am and $^{242\text{m}}\text{Am}$	37
6.4. ^{244}Cm	39
6.5. ^{243}Cm	42
6.6. ^{245}Cm	44
6.7. ^{232}U	46
7. DISCUSSION	48
8. ACKNOWLEDGMENTS	50
9. REFERENCES.	51

LIST OF FIGURES

<u>No.</u>	<u>Title</u>	<u>Page</u>
3.1.	Neutron-beam Collimator and Detector Assembly	16
3.2.	Calculated Variation in Solid Angle Subtended by All Four Hornyak Buttons When a Point Source Was Moved	17
3.3.	Ionization Chamber	17
3.4.	Block Diagram of Circuit	20
4.1.	Calibration Curve for Relative Neutron-detection Efficiency . .	25
4.2.	Counting Rate Plateau in Fission Fragment Detector	29

LIST OF TABLES

<u>No.</u>	<u>Title</u>	<u>Page</u>
3.1.	Isotopic Compositions of the Standard Samples of ^{239}Pu , ^{235}U , and ^{233}U	21
4.1.	Isotopic Composition and Fission Properties of the ^{252}Cf Standard.	26
4.2.	$\bar{\nu}_p$ -values Used for the Standards	29
4.3.	Basic Data for Calibration of Neutron-detector Efficiency. . .	31
4.4.	Ratios Used in Neutron-detector-efficiency Curve	32
6.1.	Isotopic Composition and Fission Properties of ^{241}Pu Samples	34
6.2.	Measured Neutron Yield Ratios for ^{241}Pu Samples and Standards	34
6.3.	$\bar{\nu}_p$ -ratios for ^{241}Pu Relative to Standards	35
6.4.	^{241}Pu Neutron-detector Efficiency Averaged from All the Standards	35
6.5.	Summary of Measurements of $\bar{\nu}_p(^{241}\text{Pu})$	35
6.6.	Isotopic Composition and Fission Properties of ^{238}Pu Sample .	36
6.7.	Measured Neutron Yield Ratios for ^{238}Pu Sample and Standards for Most Extensive Run	36
6.8.	$\bar{\nu}_p$ -ratios for ^{238}Pu Relative to Standards for Most Extensive Run	37
6.9.	^{238}Pu Neutron-detector Efficiency Averaged from All the Standards for Most Extensive Run.	37
6.10.	^{238}Pu $\bar{\nu}_p$ -ratios and Average $\bar{\nu}_p$ -values for All the Runs. . . .	37
6.11.	Isotopic Composition and Fission Properties of Americium Samples	38
6.12.	Measured Neutron Yield Ratios for Americium and Standard Samples	38
6.13.	$\bar{\nu}_p$ -ratios for ^{241}Am and $^{242\text{m}}\text{Am}$ Relative to Standards	38
6.14.	Americium Neutron-detector Efficiency Averaged from All the Standards	39
6.15.	Summary of Measurements of $\bar{\nu}_p(^{241}\text{Am})$ and $\bar{\nu}_p(^{242\text{m}}\text{Am})$	39
6.16.	Measured Neutron Yield Ratios for ^{244}Cm Samples and Standards	40

LIST OF TABLES

<u>No.</u>	<u>Title</u>	<u>Page</u>
6.17.	$\bar{\nu}_p$ -ratios for ^{244}Cm Relative to Standards	40
6.18.	$\bar{\nu}_p(^{244}\text{Cm})$ -values Averaged from All the Standards	41
6.19.	Summary of $\bar{\nu}_p(^{244}\text{Cm})$ Measurements	41
6.20.	Isotopic Composition and Fission Properties of ^{243}Cm Samples	42
6.21.	Measured Neutron Yield Ratios for ^{243}Cm Samples and Standards	43
6.22.	$\bar{\nu}_p$ -ratios for ^{243}Cm Relative to Standards	43
6.23.	$\bar{\nu}_p(^{243}\text{Cm})$ -values Averaged from all the Standards	44
6.24.	Isotopic Composition and Fission Properties of ^{245}Cm Sample.	44
6.25.	Measured Neutron Yield Ratios for ^{245}Cm Sample and Standards	45
6.26.	$\bar{\nu}_p$ -ratios for ^{245}Cm Relative to Standards	45
6.27.	$\bar{\nu}_p(^{245}\text{Cm})$ -values Averaged from All the Standards	46
6.28.	Isotopic Composition and Fission Properties of ^{232}U Sample .	46
6.29.	Measured Neutron Yield Ratios for ^{232}U Sample and Standards .	47
6.30.	$\bar{\nu}_p$ -ratios for ^{232}U Relative to Standards	47
6.31.	^{232}U Neutron-detection Efficiency Averaged from All the Standards	47
7.1.	Comparison of Experimental $\bar{\nu}_p$ -values with Semitheoreti- cally Derived Relations	49

SOME MEASUREMENTS OF PROMPT-NEUTRON
FISSION YIELD ($\bar{\nu}_p$) IN THERMAL-NEUTRON
FISSION OF ^{232}U , ^{238}Pu , ^{241}Pu , ^{241}Am ,
 $^{242\text{m}}\text{Am}$, ^{243}Cm , ^{245}Cm , AND IN
SPONTANEOUS FISSION OF ^{244}Cm

by

A. H. Jaffey and J. L. Lerner

ABSTRACT

The prompt-neutron fission yield ($\bar{\nu}_p$) has been measured in thermal-neutron fission of ^{232}U , ^{238}Pu , ^{241}Pu , ^{241}Am , $^{242\text{m}}\text{Am}$, ^{243}Cm , ^{245}Cm , and in the spontaneous fission of ^{244}Cm . These have been measured by comparison with $\bar{\nu}_p$ -values of the standards ^{233}U , ^{235}U , ^{239}Pu , and ^{252}Cf . A coincidence method was used, with fission fragments detected in an ionization chamber at close to 100% efficiency, and with fission neutrons detected using four symmetrically placed ZnS(Ag)-methyl methacrylate discs (Hornyak buttons). A small variation of neutron-detection efficiency with fission-neutron spectrum differences was calibrated with the four standard nuclides. The measured values of $\bar{\nu}_p$ are: ^{232}U , 3.130 ± 0.060 ; ^{238}Pu , 2.895 ± 0.027 ; ^{241}Pu , 2.874 ± 0.015 ; ^{241}Am , 3.219 ± 0.038 ; $^{242\text{m}}\text{Am}$, 3.264 ± 0.024 ; ^{243}Cm , 3.430 ± 0.047 ; ^{245}Cm , 3.832 ± 0.034 ; ^{244}Cm , 2.692 ± 0.024 .

1. INTRODUCTION

The measurement of average neutron yields ($\bar{\nu}$) from thermal-neutron fission was originally motivated by the need for accurate values in chain-reaction design. Indeed, the most accurate and careful measurements have been made with those nuclides of interest for use in nuclear reactors (^{233}U , ^{235}U , ^{239}Pu , and ^{241}Pu).*

However, $\bar{\nu}$ -values are also of interest in that they are a measure of the average excitation energy left in fission fragments after fission occurs. Any systematic consideration of the variation of fission properties over the (A, Z) range of the heavy elements must account for the $\bar{\nu}$ -variation.

*Though not of interest for reactor use, the spontaneously fissioning ^{252}Cf has also been extensively investigated because it is a useful primary standard; it has a high specific neutron-emission rate without the complication of requiring incident neutron beams.

We have attempted to expand the number of nuclides whose $\bar{\nu}$ -values have been measured, and to check the published values for some others. For most of these nuclides, there were limitations on the amount of material usable in a measurement. Such limitations were set either by the unavailability of larger amounts of some nuclides, or for others, by the fact that too much associated α -activity created a disturbing background in the ionization chamber. For this reason, comparative $\bar{\nu}$ -measurements appeared to be most reasonable, since it seemed unlikely that absolute measurements could be made on samples which might be $< 1 \mu\text{g}$ in size. The results reported are basically comparisons of the specific neutron yield of a measured nuclide with yields from standard substances whose specific neutron yields have been measured absolutely, or at least are known quite accurately.

Relative to notation, we make the standard distinction between $\bar{\nu}$, the average total yield of neutrons arising from fission, and $\bar{\nu}_p$, the average yield of prompt neutrons from fission. The difference ($\bar{\nu} - \bar{\nu}_p$) is the delayed-neutron fraction, which is of interest to nuclear-reactor designers, but is of less theoretical significance. Our method of measurement gives only ratios of $\bar{\nu}_p$ -values.

2. $\bar{\nu}_p$ -MEASUREMENT METHOD

2.1. General

For each nuclide, $\bar{\nu}_p$ was measured by comparison with three nuclides whose $\bar{\nu}_p$ -values have been determined absolutely with good accuracy, i.e., ^{233}U , ^{235}U , and ^{239}Pu . In some cases, ^{252}Cf was an added standard.

The value of $\bar{\nu}$ may be measured by counting both the number of fissions from a sample and the emitted fast neutrons, if the neutron-detection efficiency can be calibrated, as through the use of a fissionable nuclide of known $\bar{\nu}_p$. This method has the disadvantage of requiring correction for the background neutron counts caused by the neutron beam incident on the fissionable sample. Such corrections are feasible when the fission rate of the sample is high, so that the neutron counting rate from the sample is comparable to the background rate. However, if the fission activity of the sample is limited, either because of low cross section for fission or because the amount of available fissionable material is small, the background correction is relatively very large and measurement accuracy suffers severely.

The coincidence method reduces the interference due to neutron background. Neutron counts due to fission events are distinguishable since they occur simultaneously with the detection of fission fragments. Although the sample may cause only a small fractional increase in gross neutron count, these neutron counts are identifiable, so that measurement may be

made with relatively good accuracy. Extraneous neutron counts are still an interference, because they increase the accidental coincidence rate, but this background is relatively much smaller than the gross background effect.

In the measurements to be described, the fissionable material was mounted on a platinum plate, inserted into a gas-filled ionization chamber, and exposed to a collimated neutron beam emerging from the thermal-neutron column of the Argonne CP-5 reactor. The chamber served as a fission-fragment detector and had essentially 100% efficiency with thin samples. Near the chamber was the neutron detector, so placed as to subtend as large a solid angle as possible. This detector contained several Hornyak buttons,³¹ each a mixture of the scintillator ZnS(Ag) and methyl methacrylate polymer (Lucite). Because of the great difference in output pulse height from fast neutrons and γ rays, the latter were easily discriminated against even when present in high intensity.

Coincidences between fission fragment and neutron counts were measured. Since the coincidence measurement responded only to neutrons detected within a few microseconds of the fission process, delayed neutrons were not included; the experiment measured only $\bar{\nu}_p$, the mean prompt-neutron yield per fission, rather than $\bar{\nu}$, the mean total neutron yield.

2.2. Calculation of $\bar{\nu}_p$ from Coincidence Measurements

We consider first the simplest situation, with: (1) uniformly spread samples, (2) uniform thermal-neutron flux across the beam, (3) constant neutron-detection efficiency for neutrons originating anywhere in the sample, (4) no accidental coincidences (low fission and neutron counting rates). Let

A_F = fission counting rate

A_n^S = neutron counting rate from sample

A_n^B = background neutron counting rate

A_n = total neutron counting rate

C = coincidence counting rate

ϕ = thermal-neutron flux

σ_F = fission cross section

M = number of atoms of fissionable nuclide

ϵ_F = counting efficiency of fission-fragment detector (counts per fission)

ϵ_n = counting efficiency of neutron detector (counts per fission neutron emitted).

Then

$$A_F = [M\sigma_F\phi]\epsilon_F, \quad (2.1)$$

and, if ϵ_n is small enough,*

$$A_n^S = [M\sigma_F\phi][\bar{\nu}_p\epsilon_n]; \quad (2.2A)$$

$$A_n = A_n^S + A_n^B; \quad (2.2B)$$

$$C = [M\sigma_F\phi][\bar{\nu}_p\epsilon_n]\epsilon_F; \quad (2.3)$$

$$\mathcal{C} = C/A_F = \bar{\nu}_p\epsilon_n. \quad (2.4)$$

If \mathcal{C} is measured for nuclides \underline{A} and \underline{B} ,

$$\frac{\bar{\nu}_p(\underline{A})}{\bar{\nu}_p(\underline{B})} = \frac{\mathcal{C}_{\underline{A}}}{\mathcal{C}_{\underline{B}}} \frac{\epsilon_n(\underline{B})}{\epsilon_n(\underline{A})}. \quad (2.5)$$

If the efficiency ratios can be evaluated, $\bar{\nu}_p$ can be calculated from the $\bar{\nu}_p$ of a known nuclide. In practice, except when the beam shutter was closed (as in spontaneous-fission measurements), most of A_n was due to A_n^B , so (2.2A) was not a useful relation.

When sample spread, neutron flux, or neutron-detection efficiency are not uniform, results are less simple. Thus, let

m = number of atoms per unit area = $m(\rho, \theta)$, where ρ, θ are co-ordinates over the sample area S ;

$$\phi = \phi(\rho, \theta);$$

$$\epsilon_n = \epsilon_n(\rho, \theta);$$

$$\epsilon_F = \epsilon_F(\rho, \theta).$$

Then (2.1)-(2.4) become

$$A_F = \sigma_F \int_S \epsilon_F m \phi \, dS; \quad (2.6)$$

$$A_n^S = \bar{\nu}_p \sigma_F \int_S \epsilon_n m \phi \, dS; \quad (2.7)$$

$$C = \bar{\nu}_p \sigma_F \int_S \epsilon_F \epsilon_n m \phi \, dS; \quad (2.8)$$

*See Eq. (2.16).

$$\mathcal{C} = \frac{C}{A_F} = \bar{\nu}_p \frac{\int \epsilon_F \epsilon_n m \phi \, dS}{\int \epsilon_F m \phi \, dS}. \quad (2.9)$$

If ϵ_n is constant over the sample, \mathcal{C} reduces to (2.4) for any ϵ_F , ϕ , or m distribution. As noted in Sect. 3.2, ϵ_n was experimentally verified to be sufficiently constant over the sample dimensions used. Since the samples were thin, ϵ_F was very close to unity in all cases, and hence was also essentially constant.

2.3. The Relation of ϵ_n -magnitude to $\bar{\nu}_p$ -calculation

In (2.2A) or (2.7), we have written the probability of counting a fission neutron in the simple form $\bar{\nu}_p \epsilon_n$, where $\bar{\nu}_p$ is the mean number of fission neutrons emitted and ϵ_n is the probability that the detector creates a countable pulse.* With a fast-neutron detector like the Hornyak button, such simple addition of probabilities is valid only when \mathcal{P}_t , the probability that several neutrons from the same fission simultaneously create countable pulses, is much less than \mathcal{P}_1 , the probability that only one neutron does so. This is true only when ϵ_n is small. Thus, we require that \mathcal{P}_t be negligible.**

\mathcal{P}_t may be evaluated from some simple probability considerations.

Let

ϵ = Prob {A neutron will create a countable pulse, if emitted in fission};

k = number of neutrons emitted in one fission event;

\mathcal{P}_1 = Prob {Only one neutron creates a countable pulse};

\mathcal{P}_n = Prob {At least one neutron creates a countable pulse};

P_j = Prob { j neutrons simultaneously create a countable pulse};

$Q_j(k)$ = Prob { j neutrons simultaneously create a countable pulse, if k are emitted};

$P(k)$ = Prob { k neutrons are emitted}.

* For a neutron emitted in a fission, ϵ_n is the probability of the event: (1) the neutron enters a Hornyak button, (2) it suffers a recoil, (3) it creates a pulse at the photomultiplier output sufficiently large to count if the recording circuit is free. The event is considered to have occurred whether or not recording actually occurred (the event is not counted if another neutron has just been counted). We assume here that ϵ_n is the same for the first, second, third, etc., neutrons emitted in a single fission. When this is not true (e.g., if there is any directional correlation in successive neutron emissions), the required analysis will be more complex, but the conclusion will remain essentially the same.

** The event "simultaneously create countable pulses" means that each neutron has separately contributed a pulse at the photomultiplier output which is large enough for counting. However, since the pulses are simultaneous, the combination is counted as one event.

Since $\mathcal{P}_n = \mathcal{P}_1 + \mathcal{P}_t$, the use of the product $\bar{\nu}_p \epsilon_n$ in (2.2A) is appropriate when $\mathcal{P}_n \cong \mathcal{P}_1$, i.e., $\mathcal{P}_t \ll \mathcal{P}_1$.

Then, with K the maximum number of neutrons emitted in one fission process,

$$P_j = \sum_{k=j}^K Q_j(k) P(k). \quad (2.10)$$

It has been noted⁵⁶ that $P(k)$ is well represented as a binomial distribution:

$$P(k) = \binom{K}{k} p^k (1-p)^{K-k}, \quad (2.11)$$

where p is characteristic of the fissioning nuclide, but ranges from 0.399 for ^{252}Cf to 0.566 for ^{240}Pu . The mean value of the k -distribution is

$$\mathcal{E}(k) = \bar{\nu}_p = Kp. \quad (2.12)$$

$Q_j(k)$ is the binomial

$$Q_j(k) = \binom{k}{j} \epsilon^j (1-\epsilon)^{k-j}. \quad (2.13)$$

It is readily shown that the convolution (2.10) is the binomial distribution

$$P_j = \binom{K}{j} (p\epsilon)^j (1-p\epsilon)^{K-j}. \quad (2.14)$$

Then, $\mathcal{P}_n = 1 - \text{Prob}\{\text{No neutrons create a countable pulse}\} = 1 - \text{Prob}\{j=0\} = 1 - P_0$, or

$$\begin{aligned} \mathcal{P}_n &= 1 - [1 - p\epsilon]^K \cong Kp\epsilon \left[1 - \frac{K-1}{2} p\epsilon + \dots \right] \\ &\cong \bar{\nu}_p \epsilon \left[1 - \frac{K-1}{2} p\epsilon \right] = \bar{\nu}_p \epsilon \left[1 - \frac{1}{2} \bar{\nu}_p \epsilon + \frac{1}{2} p\epsilon \right]. \end{aligned} \quad (2.15)$$

For two nuclides with (K^I, ϵ^I, p^I) and $(K^{II}, \epsilon^{II}, p^{II})$,

$$\frac{\mathcal{P}_n^I}{\mathcal{P}_n^{II}} = \frac{\bar{\nu}_p^I \epsilon^I}{\bar{\nu}_p^{II} \epsilon^{II}} [1 - \alpha], \quad (2.16)$$

where

$$\alpha = \frac{K' - 1}{2} p' \epsilon' - \frac{K'' - 1}{2} p'' \epsilon'' = \frac{1}{2} [\bar{v}_p' \epsilon' - \bar{v}_p'' \epsilon''] + \frac{1}{2} [p'' \epsilon'' - p' \epsilon']. \quad (2.17)$$

Since $\epsilon' \approx \epsilon''$,

$$\alpha \approx \frac{1}{2} \epsilon \{ [\bar{v}_p' - \bar{v}_p''] + [p'' - p'] \}. \quad (2.18)$$

Taking maximum differences, and with $\epsilon \approx 5 \times 10^{-4}$, $\alpha_{\max} < \frac{1}{2}(5 \times 10^{-4})[1.5 + 0.17] = 4 \times 10^{-4}$, α is much smaller than the experimental error and hence may be neglected. This would not be true, however, if ϵ exceeded 1%.**

3. MEASURING APPARATUS

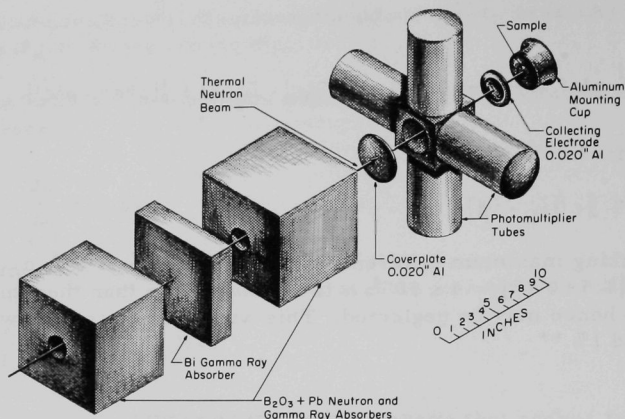
3.1. General

An ionization chamber containing the fissionable sample was placed just outside a thermal column of the Argonne CP-5 reactor. Thermal neutrons were directed into a beam with a collimator placed within the thermal column (see Fig. 3.1). Some of the graphite in back of the collimator was removed in order to increase the thermal-neutron flux ϕ . This inevitably raised the fast-neutron flux, hence the background in the neutron detector, but was unavoidable in view of the need for a higher value of ϕ . The collimator was split and a $3\frac{1}{4}$ -in.-thick aluminum-canned bismuth absorber placed between the two sections. This served greatly to decrease the γ -ray flux passing through the collimator hole, with only a corresponding fivefold decrease in thermal-neutron flux. The ionization chamber was positioned so that the beam axis was perpendicular to the sample disc.

Although it was not necessary that the flux ϕ be uniform over the sample if ϵ_n was, exploration with a small source showed ϕ to vary by $<4\%$ within an area of 10-mm radius and by $<13\%$ over an area of 16-mm radius.

* To the same order of approximation, results are similar if $P(k)$ is taken to be Poisson with mean $\mathcal{E}(k) = \bar{v}_p$. The dominant term $[\bar{v}_p' - \bar{v}_p'']$ in (2.18) remains, but the smaller term $[p'' - p']$ is absent.

** This analysis is applicable when the neutron detector is such that there is little delay between the time that a fast neutron is incident on the detector and the neutron is counted. Then two neutrons from the same fission event cannot be counted separately. However, in some neutron counters with moderators and thermal-neutron detectors, this delay may not be small. In such a counter, the several neutrons from the same fission approach thermalization at different rates and hence are countable at different times. Only a time overlap within a counter deadtime prevents the counting of each neutron that is slowed down. If the deadtime is small relative to slowing-down time, there may be little overlap in such counters even when the neutron-detection efficiency is very high. An overlap calculation analogous to the one described here must include a folding-in of the slowing-down probability distribution and the influence of counter deadtime.



121-3909

Fig. 3.1. Neutron-beam Collimator and Detector Assembly. The bismuth block strongly attenuated the γ -ray flux at only a moderate cost in neutron flux. The ionization chamber structure also served as the scintillator-photomultiplier supports.

Because the inherent sensitivity of the Hornyak button is <0.01 count per incident fission neutron, it was desired to maximize the solid angle subtended by the neutron detector at the sample. The button (and photomultiplier) were initially placed so that the detector disc was parallel to the sample disc and as close to it as possible. Since the variation of neutron-detection efficiency over the sample was dominated by solid-angle variation, such placement would also ensure the near constancy of ϵ_n , as required by (2.9).

Such positioning, however, required that both Hornyak button and photomultiplier be subject to the full blast of thermal neutrons, reactor fast neutrons, and γ rays emerging from the collimator. Although it proved possible to count under these conditions, the detector was not stable enough. The neutron-counter efficiency slowly drifted downward with increased exposure time, presumably due to photomultiplier fatigue from the many small pulses generated by the intense γ -ray flux.

3.2. Constancy of ϵ_n over the Sample

In a modification of the system, both Hornyak button and photomultiplier were placed outside of the beam. The use of four identical neutron detectors (see Fig. 3.1) surrounding the sample served to restore some of the solid angle lost in the modification, and to reduce the variation of detection efficiency over the sample. Figure 3.2 illustrates the (calculated) variation in solid angle subtended at the combination of four detectors.

Although the sample-carrying cups (see Fig. 3.3) were such as to place every sample plane at the same position, curve C shows that this positioning was not critical. Curves A and B show that the solid angle varied less than 1% over a sample whose radius was <5.5 mm. This constancy was experimentally checked with measurements made with a small ^{252}Cf source placed at a number of positions in the sample plane. \mathcal{C} was found to remain constant within statistical counting error ($\pm 1\%$) out to a radius of 10 mm in all directions.

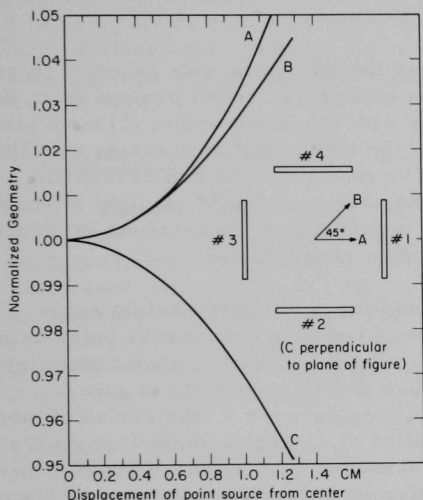
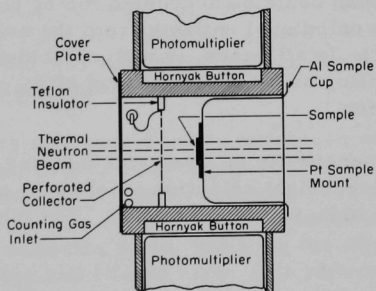


Fig. 3.2

Calculated Variation in Solid Angle Subtended by All Four Hornyak Buttons When a Point Source Was Moved. Curves A and B represent points in the plane of the sample. Curve C shows the effect of moving the source perpendicular to the usual sample plane. From C, it is evident that the neutron-detection efficiency was insensitive to the exact positioning of the sample plane.

121-3983 Rev. 1

Fig. 3.3
Ionization Chamber

121-3910

All the samples used in the $\bar{\nu}_p$ -measurements lay well within this region. The areas covered varied from 1.5 to 5 mm in radius.

3.3. Neutron Detector

The Hornyak button was made by thoroughly mixing RCA scintillator-grade ZnS(Ag) with dried ultrafine acrylic (Lucite) in the respective weight ratio 3 to 20. Both substances were in the form of very fine powders (about 300 mesh). The mixture was molded in a die at raised temperature and pressure, and then machined to the final thickness. Tests indicated that 3-mm-thick crystals gave optimum results, and these were used in the experiment.* This scintillator gave very good discrimination against the intense beam of reactor γ rays.

The Hornyak-button output pulses varied over a wide range of pulse height, because: (1) for a given neutron energy, the recoil protons from the methacrylate's hydrogen vary in energy with the recoil angle, (2) for a given recoil-proton energy, the path length in the ZnS scintillator varies with the distance between the point of origin of the recoil and the ZnS crystallite, (3) fission neutrons vary over a wide range of energies,** (4) light attenuation before reaching the photomultiplier depends upon the neutrons depth of penetration into the button before forming a recoil proton.

Over the useful range (i.e., beyond the small pulse-height range where γ -ray pileup occurred), the curve of counting rate versus pulse height dropped exponentially.[†] The value of ϵ_n varied with either photomultiplier voltage or pulse-selection level. Because of this sensitivity to gain or pulse-selection level, ϵ_n did not remain constant over a long series of measurements lasting several weeks. Variation of ϵ_n was an important source of error in this experiment. Frequent measurements of standard samples permitted determination of a running relative efficiency calibration, which was used to correct for ϵ_n -variation. Even with this correction, the data scatter was larger than could be accounted for by counting statistics alone, so errors were calculated entirely from the scatter of measured values (external error). In all cases, enough coincidence counts were accumulated so that the counting error was less (and often, much less) than the scatter due to ϵ_n -variation.

The sensitivity of a neutron detector could be varied either by adjusting a pulse-height selection level or by adjusting the photomultiplier gain through high-voltage variation. The four detectors were adjusted to

* This thickness gave a minimum error in the net coincidence rate. Increasing ϵ_n not only raised the true coincidence rate through increase in A_n^B , but also the accidental rate through increase in A_n^B . The minimum was a broad one, not changing much with buttons even two or three times thick.

** See, for example, Ref. 33 and Eq. (4.28).

[†] For typical curves, see Ref. 31.

equal sensitivity by varying individual photomultiplier voltages until each yielded the same counting rate from a small well-centered sample. One pulse-selector served for the joint output.

3.4. Sensitivity of Method

Measurement sensitivity was limited by the sample size available (or usable), by the fission cross section, and by the thermal-neutron flux ϕ . For most of the measurements, $\phi \approx 3 \times 10^7$ neutrons/cm²/sec. At this flux, 5 μ g of a nuclide with a 100-barn fission cross section would give about 2200 fissions/min and about 3.4 coinc/min. For such a sample, considerable counting time was needed to accumulate enough events for reasonable statistical error.

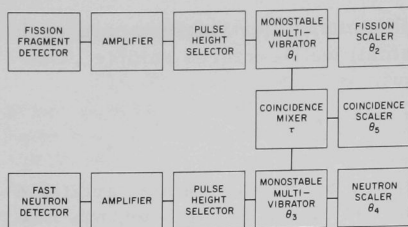
3.5. Ionization Chamber

The aluminum ionization chamber was simply constructed. The main body also served as the supporting structure for the four scintillator-photomultiplier assemblies (see Figs. 3.1 and 3.3). A Teflon-supported, perforated, thin aluminum plate allowed gas flow, and served as collecting and high-potential electrode. The aluminum sample-holding cup closed the chamber and served as the ground-potential electrode. A mixture of argon and 10% methane flowed slowly through the chamber after an initial rapid flush. The neutron beam passed from left to right in both Figs. 3.1 and 3.3.

3.6. Effect of α Pileup

One of the limiting factors in the sensitivity of the method was the amount of material usable when intense α activity was present. In order that the fission fragment-counting efficiency be kept very close to unity, it was always required that the fission counter have a good plateau before measurements were made. This was not possible when the α activity was very high, because of pulse pileup from α particles.

The allowable α activity was considerably increased when the effective dimensions of the chamber were decreased. To avoid distorting the electric field, only insulating materials were considered for construction of inserts. A thin-walled plastic cylinder was placed around the sample between sample plate and collector plate, reducing the effective chamber to a cylinder 28 mm in diameter and 10 mm high. The reduced chamber size served to decrease considerably the length of the longest α -particle tracks (parallel to the sample plate), with only a moderate loss in the lengths of the fission-fragment tracks. The small dimensions further improved the fission-fragment to α -track ionization ratio since the heaviest ionization of an α track lies near its end, whereas the fission-fragment track is most heavily ionizing near its beginning. The plastic shield had no effect upon the measured values of $\mathcal{C} = C/A_F$, but did increase the fission rate and background



121-4553

Fig. 3.4. Block Diagram of Circuit

singles counts were irrelevant. The coincidence rates were so low that the deadtime losses due to θ_5 were negligible. With the notation of Sect. 2, inclusion of deadtimes changes (2.1), (2.3), and (2.4) to

$$A_F = [M\sigma_F\phi]\epsilon_F(1 - F\theta_1); \quad (3.1)$$

$$C = [M\sigma_F\phi]\epsilon_F(1 - F\theta_1)[\bar{\nu}_p\epsilon_n][1 - A_n^B\theta_3]; \quad (3.2)$$

$$\mathcal{C} = C/A_F = \bar{\nu}_p\epsilon_n(1 - A_n^B\theta_3). \quad (3.3)$$

Since $A_n\theta_3$ was always less than 8×10^{-4} , the correction term $(1 - A_n^B\theta_3)$ was neglected, and the measured \mathcal{C} -values were taken to be related to $\bar{\nu}_p$ and ϵ_n as in (2.4). The modest deadtime losses in the fission counter thus had no effect except to change the distribution of coincidence counts from a Poisson distribution to one with a somewhat smaller ratio of (standard deviation)²/mean.*

3.8. Coincidence Time

The coincidence time τ was adjustable and was set at the minimum value that would allow counting of all true coincidences. The value of τ , approximately $1.8 \mu\text{sec}$, was empirically calibrated to good precision, since its value was used in correcting for accidental coincidences.

τ was evaluated by the following method:

a. A ^{235}U sample was counted in the usual way, yielding values of C , A_F , and A_n .

b. Another ^{235}U sample was fastened to the back of the same sample cup and hence very close to the other sample. The neutron-counting efficiency was thus the same as for the first sample, but being outside the chamber, it provided no fission-fragment counts. A measurement from

count of neutrons, because of the in-scattering of thermal neutrons by the shield, and out-scattering of fast reactor neutrons.

3.7. Circuitry. Resolution Losses

A block diagram of the circuitry is shown in Fig. 3.4. The fixed deadtimes of the multivibrators exceeded those of the scalers ($\theta_1 > \theta_2$, $\theta_3 > \theta_4$), so that scaler deadtimes for

*Although this changed the usual (Poisson) calculation of "error = [number of counts]^{1/2}," the change had no effect upon final error calculations, since these were based entirely upon data scatter.

both samples together yielded values C' , A_F' , and A_n' . Since the second sample was larger than the first, A_n' was larger than A_n and arose mostly from noncoincident counts.

Then:

$$C = A_F \epsilon_n \bar{\nu}_p + 2\tau A_n^B A_F; \quad (3.4)$$

$$C' = A_F' \epsilon_n \bar{\nu}_p + 2\tau A_n^{B'} A_F', \quad (3.5)$$

where $2\tau A_n^B A_F$ represents the accidental coincidences arising from uncorrelated fission and neutron counts.*

Then

$$2\tau = \frac{\frac{C'}{A_F'} - \frac{C}{A_F}}{A_n^{B'} - A_n^B}. \quad (3.6)$$

Now $A_n^{B'} \gg A_n^{S'} \cong A_n^S$, so that, very closely,

$$A_n' - A_n = A_n^{B'} - A_n^B \quad (3.7)$$

and

$$2\tau = \frac{\frac{C'}{A_F'} - \frac{C}{A_F}}{A_n' - A_n}. \quad (3.8)$$

3.9. Standard Samples

The standard samples were prepared in the same manner as the unknowns (see Sect. 5). The isotopic compositions of the ^{239}Pu , ^{235}U , and ^{233}U samples are shown in Table 3.1: the ^{252}Cf composition is given in

TABLE 3.1. Isotopic Compositions of the Standard Samples of ^{239}Pu , ^{235}U , and ^{233}U

^{239}Pu		^{235}U		^{233}U	
Isotope	Atom Percent	Isotope	Atom Percent	Isotope	Atom Percent
^{239}Pu	100.00	^{234}U	1.095 ± 0.004	^{233}U	98.22 ± 0.01
^{240}Pu	<0.008	^{235}U	93.44 ± 0.02	^{234}U	0.137 ± 0.001
		^{236}U	0.0054 ± 0.0003	^{235}U	0.019 ± 0.001
		^{238}U	5.46 ± 0.02	^{238}U	1.62 ± 0.01

*Strictly speaking, since only the uncorrelated events enter into the calculation of accidentals, the number of coincident events should be subtracted from A_F as well, i.e., the last term in (3.4) should be $2\tau A_n^B (A_F - A_F \epsilon_n \bar{\nu}_p)$. However, since $\epsilon_n \bar{\nu}_p \cong 1.5 \times 10^{-3}$, it may be neglected in this calculation. The tolerable fractional error in estimating 2τ is much larger than 10^{-3} .

Table 4.1 below. Three to four samples were used of each standard. Although the ^{235}U and ^{233}U samples were not isotopically pure, the thermal-fission properties were essentially those of pure samples.

4. CALCULATIONS, CORRECTIONS, AND SYSTEMATIC EFFECTS

4.1. Correction for Accidentals

Measurement yielded the coincidence rate and the singles rate from the fission and neutron detectors. It was necessary to subtract the accidental coincidences from the measured coincidence rate to yield the true fission fragment-fission neutron coincidence rate: From (2.1), (2.2), and (2.3), with* $A_F^0 = M\sigma_F\phi$,

$$A_F = A_F^0 \epsilon_F; \quad (4.1)$$

$$A_n = A_F^0 \bar{\nu}_p \epsilon_n + A_n^B; \quad (4.2)$$

$$C_{\text{tot}} = C_{\text{true}} + C_{\text{accid}} = A_F^0 \epsilon_F \epsilon_n \bar{\nu}_p + 2\tau A_F A_n^B. \quad (4.3)$$

Solving for A_n^B , we have

$$\begin{aligned} C_{\text{true}} &= C_{\text{tot}} - 2\tau A_F A_n^B \\ &= C_{\text{tot}} - \frac{2\tau A_F}{\epsilon_F - 2\tau A_F} [\epsilon_F A_n - C_{\text{tot}}], \end{aligned} \quad (4.4)$$

or, if $\epsilon_F \approx 1$, as was the case in this experiment,

$$C_{\text{true}} = C_{\text{tot}} - \frac{2\tau A_F}{1 - 2\tau A_F} [A_n - C_{\text{tot}}]. \quad (4.5)$$

The accuracy needed in this correction was modest, since $[C_{\text{true}}/C_{\text{accid}}]$ was never < 6 and was usually larger.

The C -values referred to hereafter are the C_{true} -values, as calculated from (4.5).

4.2. Correction for Neutron-detector Drift

All $C/F = \mathcal{C}$ -values were corrected for time-dependent ϵ_n -variation with a calibration curve based on \mathcal{C} -values from the standards. During one

* In (4.3), the approximation $A_F \approx A_F - A_F \epsilon_n \bar{\nu}_p$ has been made, as in (3.4); see footnote, p. 21.

series of measurements, samples of each of the standard materials ^{233}U , ^{235}U , and ^{239}Pu were counted 20 to 30 times over a period of one to two weeks. During this time each of the standard materials suffered approximately the same distribution of ϵ_n -variation. All the \mathcal{C} -values for, say ^{239}Pu , were averaged to give $\bar{\mathcal{C}}_9$, and similarly for ^{235}U ($\bar{\mathcal{C}}_5$) and ^{233}U ($\bar{\mathcal{C}}_3$). The ratios $\bar{\mathcal{C}}_9/\bar{\mathcal{C}}_5$, $\bar{\mathcal{C}}_9/\bar{\mathcal{C}}_3$, and $\bar{\mathcal{C}}_3/\bar{\mathcal{C}}_5$ were found to be very closely the same over the many series of measurements, thus justifying the assumption that the ϵ_n -variation swept over the same distribution of values for each of the standard materials.

For each ^{239}Pu \mathcal{C} -value, the efficiency ratio $\gamma_i = \mathcal{C}_i/\bar{\mathcal{C}}_9$ was evaluated, and similarly for ^{235}U and ^{233}U \mathcal{C} -values. For most of the series of measurements, γ_i varied less than $\pm 3\%$ around 1.00, although the variation in some series was as large as $\pm 6\%$. A best-fitting plot of all the γ 's against time served as the calibration curve. Every measured \mathcal{C} -value, standard as well as unknown, was then corrected to values of $\mathcal{C}_j^* = \mathcal{C}_j/\Gamma_j$, where Γ_j was the calibration factor taken from the curve. In general, for \mathcal{C}_j -values from standard samples, $\Gamma_j \neq \gamma_j$, since Γ_j was the value taken from the smoothed curve.

4.3. Averaging

The \mathcal{C}_j^* -values for each nuclide were averaged as $\bar{\mathcal{C}}^*$ and used in Eq. (2.5) for calculating $\bar{\nu}_p$ -ratios. Thus, for one nuclide, for n measurements,

$$\bar{\mathcal{C}}^* = \frac{1}{n} \sum_{j=1}^n \mathcal{C}_j^*. \quad (4.6)$$

The error in \mathcal{C}^* was calculated in the usual way, with

$$s^2(\mathcal{C}_j^*) = \frac{1}{r} \sum_{j=1}^n (\mathcal{C}_j^* - \bar{\mathcal{C}}^*)^2, \quad (4.7)$$

and the error in the mean as

$$s(\bar{\mathcal{C}}^*) = s(\mathcal{C}_j^*)/\sqrt{n}. \quad (4.8)$$

For an unknown nuclide, the usual relation $r = n - 1$ holds. For a standard nuclide, on the other hand, r was somewhat smaller than $n - 1$, because of correlation effects. Correlation was introduced by the fact that the calibration curve was in part determined by γ -values from the same standard. Such correlation is minimal when the calibration curve is

monotonic (e.g., a straight line), and increases with the number of maxima and minima in the curve.* We used $r = n - 1 - \kappa f$, where f is the estimated degrees of freedom lost (in the least-squares sense) due to the structure of the calibration curve;** $\kappa = c/d$, with d the total number of γ -values used in forming the calibration curve, and c the number of γ -values derived from the particular standard considered. Very conservatively f was taken as four times the number of extrema (maxima or minima) or points of inflection in the curve.

4.4. Correction for Other Fissioning Isotopes

For most of the measurements, it was not possible to prepare samples in which only the "unknown" nuclide was fissionable with thermal neutrons. When other fissionable isotopes were present, correction for their effect required that we know their $\bar{\nu}_p$ -values, their concentrations relative to the "unknown" isotope, and the relative numbers of fissions from the various isotopes.

For the isotopes X, v, w,

$$C_{Xvw} = \epsilon_{nX} \bar{\nu}_{pX} A_{FX} + \epsilon_{nv} \bar{\nu}_{pv} A_{Fv} + \epsilon_{nw} \bar{\nu}_{pw} A_{Fw}; \quad (4.9)$$

$$A_F = A_{FX} + A_{Fv} + A_{Fw}. \quad (4.10)$$

With $f_X = A_{FX}/A_F$, etc.,[†]

$$\mathcal{C}_{Xvw} = C_{Xvw}/A_F = \epsilon_{nX} \bar{\nu}_{pX} f_X + \epsilon_{nv} \bar{\nu}_{pv} f_v + \epsilon_{nw} \bar{\nu}_{pw} f_w. \quad (4.11)$$

If $\bar{\nu}_{pX}$ is the unknown and measurements are made relative to a standard S, then

$$\frac{\mathcal{C}_{Xvw}}{\mathcal{C}_S} = \frac{\epsilon_{nX} \bar{\nu}_{pX} f_X}{\epsilon_{nS} \bar{\nu}_{pS}} + \frac{\epsilon_{nv} \bar{\nu}_{pv} f_v}{\epsilon_{nS} \bar{\nu}_{pS}} + \frac{\epsilon_{nw} \bar{\nu}_{pw} f_w}{\epsilon_{nS} \bar{\nu}_{pS}} \quad (4.12)$$

or

$$\frac{\bar{\nu}_{pX}}{\bar{\nu}_{pS}} = \left(\frac{\epsilon_{nS}}{\epsilon_{nX}} \right) \left[\frac{\mathcal{C}_{Xvw}}{\mathcal{C}_S} \frac{1}{f_X} - \left(\frac{\epsilon_{nv}}{\epsilon_{nS}} \right) \frac{\bar{\nu}_{pv}}{\bar{\nu}_{pS}} \frac{f_v}{f_X} - \left(\frac{\epsilon_{nw}}{\epsilon_{nS}} \right) \frac{\bar{\nu}_{pw}}{\bar{\nu}_{pS}} \frac{f_w}{f_X} \right]. \quad (4.13)$$

* In a straight-line fit, a single γ -value has minimal effect on the local behavior of the calibration curve.

With an increasing number of up-and-back turns, a single γ -value has less and less effect upon the distant behavior of the fitted curve, and has more and more effect upon the local behavior.

** This relation was based upon a theoretical analysis of simple cases and a sampling (Monte Carlo) calculation for several more complicated variations of a calibration curve.³⁶

[†] Hereafter, when the term \mathcal{C}_i is used, it refers to the drift-corrected average value, as in Eq. (4.6).

If only two fissionable isotopes are present, this becomes

$$\frac{\bar{\nu}_{pX}}{\bar{\nu}_{pS}} = \left(\frac{\epsilon_{nS}}{\epsilon_{nX}} \right) \frac{\mathcal{C}_{Xv}}{\mathcal{C}_S} + \frac{f_v}{f_X} \left[\left(\frac{\epsilon_{nS}}{\epsilon_{nX}} \right) \frac{\mathcal{C}_{Xv}}{\mathcal{C}_S} - \left(\frac{\epsilon_{nv}}{\epsilon_{nX}} \right) \frac{\bar{\nu}_{pv}}{\bar{\nu}_{pS}} \right], \quad (4.14)$$

where $f_v = 1 - f_X$. If isotope v is also the standard S ,

$$\frac{\bar{\nu}_{pX}}{\bar{\nu}_{pS}} = \left(\frac{\epsilon_{nS}}{\epsilon_{nX}} \right) \left[\frac{\mathcal{C}_{Xv}}{\mathcal{C}_S} + \frac{f_v}{f_X} \left\{ \frac{\mathcal{C}_{Xv}}{\mathcal{C}_S} - 1 \right\} \right]. \quad (4.15)$$

The ratios (f_X, f_v, f_w) were calculated from the known mass ratios and the known fission cross sections for thermal neutrons.

4.5. Averaging Results Relative to the Three Standards

The relations (4.13)-(4.15) are useful for calculating the ratio of $\bar{\nu}_{pX}$ to $\bar{\nu}_p$ of the standards. If the accepted $\bar{\nu}_p$ -value of each standard is entered into the corresponding ratios, three values of $\bar{\nu}_{pX}$ emerge. If these are averaged, error estimation must allow for the correlation introduced by using the same value of \mathcal{C}_{Xvw} in each ratio. This correlation effect is readily evaluated.

In an alternative averaging procedure, the measurements on the standards are averaged to evaluate ϵ_{nX} , and \mathcal{C}_{Xvw} is used only once.

We let the three standards ^{235}U , ^{233}U , and ^{239}Pu be numbered 1, 2, and 3, and use all three \mathcal{C} -values to calculate ϵ_{nS} . Thus,

$$\epsilon_1 = \mathcal{C}_1 / \bar{\nu}_{p1}; \quad \epsilon_2 = \mathcal{C}_2 / \bar{\nu}_{p2}; \quad \epsilon_3 = \mathcal{C}_3 / \bar{\nu}_{p3} \quad (4.16)$$

are evaluated from the measured \mathcal{C} -values of the standards and their known $\bar{\nu}_p$ -values. These provide independent estimates of ϵ_{nX} through use of ϵ -ratios taken from Fig. 4.1:

$$(\epsilon_{nX})_1 = \epsilon_1 \left(\frac{\epsilon_{nX}}{\epsilon_1} \right); \quad (\epsilon_{nX})_2 = \epsilon_2 \left(\frac{\epsilon_{nX}}{\epsilon_2} \right); \quad (\epsilon_{nX})_3 = \epsilon_3 \left(\frac{\epsilon_{nX}}{\epsilon_3} \right). \quad (4.17)$$

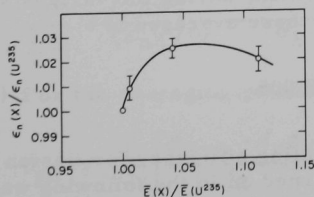


Fig. 4.1

Calibration Curve for Relative Neutron-detection Efficiency. A preliminary $\bar{\nu}_p$ -value $\bar{\nu}_{pX}$ yields the mean neutron energy \bar{E}_X through Eq. (4.31). The relative detection efficiency $\epsilon_n(X)/\epsilon_n(^{235}\text{U})$ is then read from the curve.

We take $\bar{\epsilon}_{nX}$ as the average of $(\epsilon_{nX})_1$, $(\epsilon_{nX})_2$, and $(\epsilon_{nX})_3$. From Eq. (4.11), we have

$$\bar{\nu}_{pX} = \frac{1}{\bar{\epsilon}_{nX} f_X} \mathcal{C}_{Xvw} - \left(\frac{\epsilon_{nv}}{\epsilon_{nX}} \right) \left(\frac{f_v}{f_X} \right) \bar{\nu}_{pv} - \left(\frac{\epsilon_{nw}}{\epsilon_{nX}} \right) \left(\frac{f_w}{f_X} \right) \bar{\nu}_{pw} \quad (4.18)$$

with ϵ -ratios taken from Fig. 4.1. With only two isotopes,

$$\bar{\nu}_{pX} = \frac{\mathcal{C}_{Xv}}{\bar{\epsilon}_{nX}} + \frac{f_v}{f_X} \left[\frac{\mathcal{C}_{Xv}}{\bar{\epsilon}_{nX}} - \left(\frac{\epsilon_{nv}}{\epsilon_{nX}} \right) \bar{\nu}_{pv} \right]. \quad (4.19)$$

Another correlation effect in error calculation applies to both methods of averaging and is described at the end of Sect. 4.9.

4.6. Correction for a Spontaneously Fissioning Isotope

In some cases, the interfering isotope was not thermally fissionable, but did undergo spontaneous fission. In such a case, it was possible to correct for this isotope by measuring \mathcal{C} with the thermal-neutron beam absent (beam shutter closed). To calibrate the difference in ϵ_n for the spontaneously fissionable isotope with and without the thermal-neutron beam present, \mathcal{C} was evaluated with a ^{252}Cf sample, for which the spontaneous fission rate greatly exceeded the rate of thermal-neutron fission (see Table 4.1). A beam-generated ϵ_n -shift could thus be calibrated by measuring with and without the thermal-neutron beam.

TABLE 4.1. Isotopic Composition and Fission Properties of the ^{252}Cf Standard^a

	Atom Percent	Half-life for Spontaneous Fission (yr) (Ref. 32)	Specific Activity from Spontaneous Fission (fissions/min/ μg)	Fission Cross Section ^b (Ref. 32)	Thermal Neutron Fission Activity ^b in Neutron Flux [fissions/min]	Spontaneous Fission Activity ^b [fissions/min]
^{249}Cf	8.8	6.87×10^{10}	0.046	1735	660	<1
^{250}Cf	20.7	1.73×10^4	1.85×10^5	<350	<300	0.004×10^7
^{251}Cf	7.6	-	-	3000	990	-
^{252}Cf	62.9	85.5	3.7×10^7			2.3×10^7

^aIn this sample [spontaneous fissions/thermal-neutron fission] > 10^4 .

^bFrom total of 1 μg of californium, in a flux $\phi = 3 \times 10^7$ neutrons/cm²/sec.

Twenty-six such comparisons were made during the various series of measurements described in Sect. 6, and these averaged to

$$^{252}\text{Cf: } R = \frac{\mathcal{C}[\text{beam on}]}{\mathcal{C}[\text{beam off}]} = 1.038 \pm 0.005. \quad (4.20)$$

We may explain the increase in counting efficiency for fission neutrons when the thermal-neutron beam is turned on in the following way:

When the reactor beam hits the sample, a high flux of γ rays is scattered into the neutron detector. These gammas create many very small pulses whose pileup is well below the selection level; however, the pileup, in effect, creates an increased "noise level" or baseline, with larger positive and negative excursions than occur in the absence of the beam. A pulse generated by a fission neutron has as much chance of hitting a "noise" peak as a valley. Some neutron pulses [Type A] which are intrinsically just below the selection level may superimpose upon a "noise" peak and be counted; other neutron pulses [Type B] which are intrinsically just above the selection level may superimpose upon a "noise" valley and not be counted. However, these two classes do not compensate for each other. Because the pulse-height distribution drops off exponentially, there are more Type A than Type B events; hence, the net counting rate is increased.

To calculate the correction for a spontaneously fissioning isotope, we start with Eq. (4.11). For the spontaneous fission alone (beam off) of, say, the v -isotope, measurement yields

$$\mathcal{C}'_v = \epsilon'_{nv} \bar{\nu}_{pv}, \quad (4.21)$$

where ϵ'_{nv} is the neutron-counter efficiency for isotope v with the neutron beam off. Taking $\epsilon_{nv} = R\epsilon'_{nv}$, with R in Eq. (4.20), \mathcal{C}'_v is corrected to the value it would have had if measured by itself in the thermal beam. Thus,

$$\mathcal{C}_v = R\mathcal{C}'_v = \epsilon_{nv} \bar{\nu}_{pv} \quad (4.22)$$

and

$$\mathcal{C}_{Xvw} = \epsilon_{nX} \bar{\nu}_{pX} f_X + f_v \mathcal{C}_v + \epsilon_{nw} \bar{\nu}_{pw} f_w. \quad (4.23)$$

Comparing to a standard,

$$\frac{\bar{\nu}_{pX}}{\bar{\nu}_{pS}} = \left(\frac{\epsilon_{nS}}{\epsilon_{nX}} \right) \left[\frac{1}{f_X} \frac{\mathcal{C}_{Xvw} - f_v \mathcal{C}_v}{\mathcal{C}_S} - \left(\frac{\epsilon_{nw}}{\epsilon_{nS}} \right) \frac{\bar{\nu}_{pw}}{\bar{\nu}_{pS}} \frac{f_w}{f_X} \right]. \quad (4.24)$$

With only X and v in the sample,

$$\frac{\bar{\nu}_{pX}}{\bar{\nu}_{pS}} = \left(\frac{\epsilon_{nS}}{\epsilon_{nX}} \right) \frac{1}{f_X} \frac{\mathcal{C}_{Xv} - f_v \mathcal{C}_v}{\mathcal{C}_S}. \quad (4.25)$$

For the averaging relations equivalent to Eqs. (4.18) and (4.19),

$$\bar{\nu}_{pX} = \frac{1}{\epsilon_{nX}} \left[\frac{\mathcal{C}_{Xvw} - f_v \mathcal{C}_v}{f_X} - \left(\frac{\epsilon_{nw}}{\epsilon_{nX}} \right) \frac{f_w}{f_X} \bar{\nu}_{pw} \right] \quad (4.26)$$

or, for only two isotopes present,

$$\bar{v}_{pX} = \frac{1}{\bar{\epsilon}_{nX}} \frac{C_{Xvw} - f_v C_v}{f_X} = \frac{1}{\bar{\epsilon}_{nX}} \left[C_v + \frac{C_{Xvw} - C_v}{f_X} \right]. \quad (4.27)$$

If \bar{v}_{pV} is known, (4.13) or (4.14) may be used instead of (4.24) or (4.25); similarly, (4.18) or (4.19) may be used instead of (4.26) or (4.27).

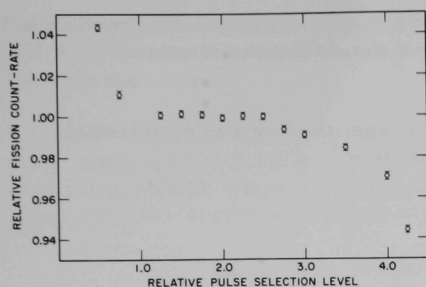
f_w is calculated, as before, from the known percentage composition of the sample, and from the known fission cross sections. On the other hand, f_v is the measured ratio: [fission rate, beam off]/[fission rate, beam on].

4.7. Effect of Directional Correlation between Fission Fragment and Fission Neutrons

A potential source of systematic error arises from the known correlation between the direction of fission fragments and the emitted fission neutrons. Because of this correlation, the neutrons detected by the Hornyak buttons come largely from those fragments which have a large velocity component parallel to the sample plate; hence, these form the fission-fragment pulses involved in most of the true coincidences measured.* When samples are "thick," such fragments tend to be stopped in the sample more frequently than fragments emitted perpendicular to the sample plate. Hence, sample self-absorption cuts the coincidence rate more than the fission rate, with a consequent decrease in $C = C/A_F$.

Because of this potential error, sample-preparation methods were designed to minimize sample self-absorption. The sample mass was small, frequently $<10 \mu\text{g}$, and prepurified (by solvent extraction and ion exchange) to remove nonactive solid. Spreading agents were used to improve the uniformity of the sample. The sample absorption effect was small, as indicated by the very small slope of the fission plateau (fission-fragment count versus pulse-height selection level, as in Fig. 4.2). To minimize the self-absorption effect, the pulse-selection level used was as low as was feasible while allowing adequate protection against pileup pulses from α -particle activity. Finally, for a number of the nuclides measured (including standards), several samples containing different amounts of the same material always gave the same values of $C = C/A_F$. Although this effect is important only if it differs between unknown and standard, the simplest way of equalizing the two effects is to make them both small.

*This effect was demonstrated experimentally. A ^{235}U sample was placed in the chamber without a surrounding plastic cylinder. Fission tracks (A) with a large velocity component in the sample plane were then able to yield full ionization, whereas tracks (B) emitted close to perpendicular to the sample yielded only the ionization from about 1 cm of track. When the fission pulse-height selection level was raised to cut the fission rate to 60% of the plateau value, Type (B) tracks were preferentially cut out. This decreased A_F more than it did C. The observed value of $C = C/A_F$ correspondingly increased by 10%.



121-4554

Fig. 4.2. Counting Rate Plateau in Fission Fragment Detector

It seems reasonable to use a midway value, $\bar{\nu}_p(^{252}\text{Cf}) = 3.764$.^{22,60} The corresponding values for the standards are given in Table 4.2.

TABLE 4.2. $\bar{\nu}_p$ -values Used for the Standards

$\bar{\nu}_p$		$\bar{\nu}_p$	
^{239}Pu	2.884 ± 0.007	^{235}U	2.407 ± 0.005
^{233}U	2.478 ± 0.007	^{252}Cf	3.764 ± 0.015

Our results are presented in terms of ratios to the standard values. The standard $\bar{\nu}_p$ -values are also used to calculate an overall averaged $\bar{\nu}_p$ -value for the unknown. Future definitive results for $\bar{\nu}_p(^{252}\text{Cf})$ will shift our reported $\bar{\nu}_p$ -values by the relative shift from the value 3.764.

4.9. Calibration of Relative Neutron-counting-efficiency Variation with Neutron-energy Spectrum

It is evident from Eq. (2.5) that it is necessary to know the relative counting efficiency for fission neutrons for the various nuclides. The $\bar{\nu}_p$ -measurements described here were possible only because the fission-neutron spectra from various nuclides are very similar, so that $\epsilon_n(\text{A})/\epsilon_n(\text{B})$ is close to unity. We calibrated this ratio over a wide range of fission-neutron spectra and found the ratio not to exceed 1.03; in most cases it was less. Avoidance of a systematic error, however, required correction for this small effect. Some interpolation method was needed to relate the spectral differences among the standards to those of the unknowns.

Conceptually, this is not as simple as one might hope for, since the theory of neutron spectra is only approximate and the measurements that have been made scatter widely. On the other hand, the correction ratios

4.8. $\bar{\nu}_p$ -values for the Standards

At the present time, there is some uncertainty as to the appropriate absolute scale for $\bar{\nu}_p$ -values of the standards. The experimental ratios of $\bar{\nu}_p$ -values agree better than the absolute values. The basic source of the discrepancies arises from the unresolved differences in measured values of $\bar{\nu}_p(^{252}\text{Cf})$. Several authors have carefully evaluated possible systematic effects in the various measurements, but the sources of discrepancies have not been isolated.

differ very modestly from unity, and even a crude interpolation method will serve adequately to tie together observed ratios for the standards and derived values for the unknowns.

Over a large part of the energy range, the neutron distribution is fitted quite closely by the gamma distribution⁵⁷

$$N(E) dE = \frac{1}{\Gamma(\frac{3}{2})} \frac{1}{T^{\frac{3}{2}}} E^{\frac{1}{2}} e^{-E/T} dE, \quad (4.28)$$

where $\Gamma(\frac{3}{2}) = \frac{1}{2}\sqrt{\pi}$. The mean energy value is

$$\bar{E} = \int_0^{\infty} E N(E) dE = \frac{3}{2} T. \quad (4.29)$$

Since the $N(E)$ distributions almost completely overlap, the corresponding \bar{E} -values do not differ much. Thus the ϵ_n -values are almost the same for various nuclides.

The relative \mathcal{O} -values for the standard nuclides ^{233}U , ^{235}U , ^{239}Pu , and ^{252}Cf were used to calibrate an ϵ_n -curve. From Eq. (2.4),

$$\frac{\epsilon_n(^{233}\text{U})}{\epsilon_n(^{235}\text{U})} = \frac{\mathcal{O}(^{233}\text{U})/\mathcal{O}(^{235}\text{U})}{\bar{\nu}_p(^{233}\text{U})/\bar{\nu}_p(^{235}\text{U})}. \quad (4.30)$$

The numerator on the right side is derived from the ratios averaged over all the experiments. The denominator comes from the known experimental values of $\bar{\nu}_p$ (see Table 4.2). The ratios $\epsilon_n(^{239}\text{Pu})/\epsilon_n(^{235}\text{U})$ and $\epsilon_n(^{252}\text{Cf})/\epsilon_n(^{235}\text{U})$ were similarly evaluated. Experimental \mathcal{O} -ratios and standard $\bar{\nu}_p$ -ratios are shown in Table 4.3, and corresponding values of $\epsilon_n(X)/\epsilon_n(^{235}\text{U})$ are listed in Table 4.4.

The ϵ_n -ratios differ slightly from unity because of moderate differences in the $N(E)$ distributions. For purposes of interpolation, it is convenient to plot these ratios against ratios of the parameter characterizing $N(E)$, i.e., $\bar{E} = \frac{3}{2} T$. Because experimental \bar{E} -values scatter widely (see Table 4.4), we preferred to use a semitheoretical relation:^{57, 58, 59}

$$\bar{E} = 0.75 + 0.65(\bar{\nu} + 1)^{\frac{1}{2}}, \quad (4.31)$$

which approximately averages the discordant \bar{E} -results. Values are shown in Table 4.4. Since the variation in the ϵ_n -ratio is so small, the general validity of Eq. (4.31) or even of Eq. (4.28) is not important; only the monotonicity of \bar{E} with $\bar{\nu}_p$ determines the usefulness of the relation in forming

the calibration curve (see Fig. 4.1). In using Fig. 4.1, errors in the ϵ_n -ratio due to uncertainty in the \bar{E} -ratios were less than the experimental error in drawing the curve.

For calculating $\bar{\nu}_p$ -ratios, ϵ_n -ratios were read from this curve. An error allowance of 0.7% in the ϵ_n -ratio was made whenever Fig. 4.1 was used for a nuclide whose $\bar{\nu}_p$ (hence \bar{E}) was not close to that of a standard. Otherwise, the errors in Table 4.4 were used.

TABLE 4.3. Basic Data for Calibration of Neutron-detector Efficiency

Nuclides	ϵ -ratios ^a	$\bar{\nu}_p$ -ratios ^b	References for $\bar{\nu}_p$ -ratio
$\frac{^{233}\text{U}}{^{235}\text{U}}$	1.039 ± 0.002	1.030 ± 0.004	22 ^c
$\frac{^{239}\text{Pu}}{^{235}\text{U}}$	1.229 ± 0.003	1.199 ± 0.004	22 ^c
$\frac{^{252}\text{Cf}}{^{235}\text{U}}$	1.591 ± 0.008	1.553 ± 0.019	44
		1.555 ± 0.013	30
		1.568 ± 0.008	43
		1.562 ± 0.013	14
		1.559 ± 0.004	60 ^d
		1.557 ± 0.007	12, 13
		1.557 ± 0.023	18, 49
		1.562 ± 0.011	45
		1.563 ± 0.007	6
	average	1.560 ± 0.002	

^aAveraged from values measured in all the experiments described in Sect. 6.

^bTaken from cited literature. Where $\bar{\nu}$ is given instead of $\bar{\nu}_p$, correction is made for the delayed-neutron fraction.³⁴

^cA survey and least-squares averaging.

^dThis is a least-squares summary and includes some of the other results cited; it is used here because it also includes other measurements.

TABLE 4.4. Ratios Used in Neutron-detector-efficiency Curve

X	$\frac{\epsilon_n(X)}{\epsilon_n(^{235}\text{U})}$ ^a	$\frac{\bar{E}(X)}{\bar{E}(^{235}\text{U})}$ ^b (semitheoretical)	$\frac{\bar{E}(X)}{\bar{E}(^{235}\text{U})}$ Experimental	References for Previous Column
²³⁵ U	1.000	1.000	1.000	
²³³ U	1.009 ± 0.005	1.006	1.031 ± 0.008	38
			0.958 ± 0.020	54
			1.018 ± 0.003	8
			1.015 ± 0.036	58 ^c
			1.021 ± 0.005	25
²³⁹ Pu	1.025 ± 0.004	1.041	1.038 ± 0.008	38
			1.040 ± 0.003	8
			1.085 ± 0.030	2
			1.041 ± 0.036	58 ^c
			1.088 ± 0.047	15
²⁵² Cf	1.020 ± 0.005	1.112	1.039 ± 0.002	25
			1.186	53
			1.026 ± 0.032	8
			1.200 ± 0.041	9 ^d
			1.103 ± 0.050	58 ^c
²⁴⁴ Cm		1.025 ^e	1.121 ± 0.048	15
			1.189	52
			1.121 ± 0.012 ^f	26

^aCalculated from Eq. (4.30) from values in Table 4.3.

^bCalculated from Eq. (4.31).

^cA review, not an independent measurement.

^dCombined with average $\bar{E}(^{235}\text{U})$ -value taken from a review.⁵⁸

^eBased upon a $\bar{\nu}_p$ -value of 3.69.

^fThis number was calculated by the authors, and not by Herold. We wish to thank him for providing us with the original data, from which we made a least-squares fit to Eq. (4.28). This gave $T = 1458 \pm 6.2$ keV or $\bar{E} = 2.187 \pm 0.009$ MeV. The fit was quite good except that from 0.5 to 0.9 MeV observations lay systematically 1 to $1\frac{1}{2}$ standard deviations below the fitted curve. Since no measurements were made of $\bar{E}(^{235}\text{U})$, we have normalized the result to $\bar{E}(^{235}\text{U}) = 1.95 \pm 0.02$. The ratio is clearly higher than that expected from Eq. (4.31).

The use of Fig. 4.1 to provide ϵ_n -ratios for calculating (4.18) or (4.19) introduces a correlation in evaluating the statistical error in the final $\bar{\nu}_p$ -value. The efficiencies ϵ_n for each standard nuclide (S_i) are calculated using the literature value of each $\bar{\nu}_p(S_i)$, as in Eq. (4.16). Each $\epsilon_n(S_i)$ is then used to calculate $\epsilon_n(X)$, using Fig. 4.1. The average $\bar{\epsilon}_n(X)$ is then used to calculate $\bar{\nu}_p(X)$, as in Eq. (4.19). Since each $\bar{\nu}_p(S_i)$ is used twice, once in Eq. (4.16) and then in Eq. (4.17), a correlation is introduced which affects the error calculation of $\bar{\epsilon}_n(X)$. In every case, the quoted error includes the effect of this correlation.

*Details are omitted here since the algebra is lengthy. The correlations are readily calculated by the approximate methods used for calculating the usual propagation of errors formulae. The magnitude of the correlation effect depends upon the relative magnitudes of the errors in \mathcal{C}_i and $\bar{\nu}_p(S_i)$.

5. MEASUREMENTS

Samples were all mounted in much the same way. A small volume of a solution containing the fissionable material was evaporated on a 25-mm-dia platinum disc of 0.05-mm thickness. In most cases, the material had already been separated from other elements with an ion-exchange column. Extraneous solids were minimal. Some of the standard samples were electroplated, rather than evaporated; both kinds gave the same values of $\mathcal{C} = C/A_F$. The areas of spread were kept at less than a 5-mm radius, and the average sample thickness varied from 5 to 40 $\mu\text{g}/\text{cm}^2$. Spreading agents were used to prevent clumping and to improve sample thickness uniformity. For each sample, final proof of adequate uniformity was achieved when measurement showed the fission-counter plateaus to be quite flat, indicating that ϵ_F was close to unity. A sample yielding a poor plateau was dissolved, purified, and redeposited: it was not considered acceptable unless it yielded a flat plateau.

Each platinum disc was cemented to a cup spun from thin aluminum, taking care that the deposit (not the disc) was centered on the cup. Such a cup, when mounted in the chamber (see Fig. 3.2), served (1) to place the sample at the geometric center of the neutron-detector array, (2) to place the sample at a 1-cm distance from the collecting electrode of the ionization chamber, (3) to seal the chamber so that the slowly flowing gas could be controlled in flow, and (4) as the second electrode of a parallel-plate ion chamber. As a check on centering, $\mathcal{C} = C/A_F$ was measured with the cup rotated at various angular positions relative to the four Hornyak buttons. Measurement continued only if \mathcal{C} remained constant.

Samples were counted in sequence, unknown samples along with standards prepared from ^{239}Pu , ^{233}U , ^{235}U , and in some measurement series ^{252}Cf . Counts of the standards served the dual purpose of allowing the comparison of $\bar{\nu}_p$ -values as well as calibrating the drift in counting efficiency of the fast-neutron detector. Because of the necessity for calibrating the ϵ_n -variation, more time was devoted to counting of standards than to the unknowns. Several samples of each standard material were used, and each standard material was measured 15 to 30 times in a series of measurements.

The τ -value of the coincidence circuit was redetermined at intervals, but proved to be quite constant.

6. MEASUREMENTS AND RESULTS

6.1 ^{241}Pu

Two samples were used: one (I) was formed by a high-burnup irradiation of ^{239}Pu ; the other (II) was received from the Oak Ridge Isotope Separation Division. The isotopic compositions of the samples at the time

of the $\bar{\nu}_p$ -measurement are shown in Table 6.1. The ^{241}Pu content in (I) was corrected for decay during 1.75 yr between mass-spectrometric analysis and $\bar{\nu}_p$ -measurement, using the Oetting and Gunn half-life $T_{1/2} = 14.03 \pm 0.3$ yr. The uncertainty in the ^{241}Pu half-life has a negligible effect on the $\bar{\nu}_p$ -results, because the amount of decay is $<10\%$ and because $\bar{\nu}_p$ of the interfering isotope (^{239}Pu) is close to that of ^{241}Pu .

TABLE 6.1. Isotopic Composition and Fission Properties of ^{241}Pu Samples

	Atom Percent		Half-life ⁴¹ (yr)	Spontaneous Fission Half-life ³² (yr)	Specific Activity from Spontaneous Fission [fissions/min/μg]	Effective Thermal Fission Cross Section (barn)
	Sample I	Sample II				
^{238}Pu		0.0166 ± 0.0008	86	5×10^{10}	0.068	18.3 ± 5^{32}
^{239}Pu	5.33 ± 0.05	26.2 ± 0.3	24,400			788 ± 5^a
^{240}Pu	39.0 ± 0.4	13.7 ± 0.2	6,580	1.34×10^{11}	0.025	$<0.05^{32}$
^{241}Pu	19.8 ± 0.3	59.4 ± 0.4	14.03 ± 0.3^{48}			1061 ± 11^b
^{242}Pu	34.1 ± 0.3	0.671 ± 0.006	379,000	6.5×10^{10}	0.05	$<0.3^{32}$
^{244}Pu	0.0018 ± 0.0001			2.5×10^{10}	0.13	

^a $\sigma_F(0.0253 \text{ eV})^{60}$ and g_F^{61} .

^b $\sigma_F(0.0253)^{60}$ and g_F^{42} .

TABLE 6.2. Measured Neutron Yield Ratios for ^{241}Pu Samples and Standards

	$\bar{\epsilon}^* \pm s(\bar{\epsilon}^*) [\times 10^3]$
^{239}Pu	1.789 ± 0.006
^{235}U	1.462 ± 0.004
^{233}U	1.535 ± 0.010
^{241}Pu (I)	1.789 ± 0.007
^{241}Pu (II)	1.788 ± 0.006

As compared to the neutron-induced fission rates of ^{239}Pu and ^{241}Pu , the spontaneous fission rates of ^{240}Pu and ^{242}Pu were negligible.

After correction for drift (see Sect. 4.2), the average values of $\mathcal{C} = C/A_F$ are given in Table 6.2; the indicated error is taken from Eq. (4.8).

Calculation of the relative $\bar{\nu}_p$ -values requires correction for ^{239}Pu fission. From Eq. (4.14),

$$\frac{\bar{\nu}_p(^{241}\text{Pu})}{\bar{\nu}_p(S)} = \frac{\epsilon_n(S)}{\epsilon_n(^{241}\text{Pu})} \frac{\bar{\epsilon}^*(^{241}\text{Pu})}{\bar{\epsilon}^*(S)} + \frac{f(^{239}\text{Pu})}{f(^{241}\text{Pu})} \times \left[\frac{\epsilon_n(S)}{\epsilon_n(^{241}\text{Pu})} \frac{\bar{\epsilon}^*(^{241}\text{Pu})}{\bar{\epsilon}^*(S)} - \frac{\epsilon_n(^{239}\text{Pu})}{\epsilon_n(^{241}\text{Pu})} \frac{\bar{\nu}_p(^{239}\text{Pu})}{\bar{\nu}_p(S)} \right].$$

Since $\bar{\nu}_p(^{241}\text{Pu})$ is very close to that of ^{239}Pu , from Eq. (4.28) we may take $\epsilon_n(^{239}\text{Pu}) = \epsilon_n(^{241}\text{Pu})$. The relative fission rate $A_F(^{239}\text{Pu})/A_F(^{241}\text{Pu})$ is derived from the effective cross-section ratio and the atomic percent (see Table 6.1). For (I), $f(^{239}\text{Pu})/f(^{241}\text{Pu}) = 0.218 \pm 0.004$, and for (II) the ratio is 0.357 ± 0.005 . Errors in these ratios have little effect, since $\bar{\nu}_p(^{241}\text{Pu})$ is so close to $\bar{\nu}_p(^{239}\text{Pu})$. $\bar{\nu}_p$ -ratios are given in Table 6.3. Because $\bar{\nu}_p(^{241}\text{Pu})$ is very close to $\bar{\nu}_p(^{239}\text{Pu})$, the correction involving $f(^{239}\text{Pu})/f(^{241}\text{Pu})$ is small. For averaging $\bar{\nu}_p$ -values calculated from each standard

we use Eqs. (4.17) and (4.19), as in Table 6.4. $\epsilon_n(^{241}\text{Pu})$, inserted into Eq. (4.19), yields $\bar{\nu}_p(^{241}\text{Pu}) = 2.874 \pm 0.015$. The quoted error includes only the statistical error.

TABLE 6.3. $\bar{\nu}_p$ -ratios for ^{241}Pu Relative to Standards

S	$\frac{\bar{\nu}_p(^{241}\text{Pu})}{\bar{\nu}_p(\text{S})}$		
	Sample I	Sample II	Average
^{239}Pu	1.000 ± 0.005	0.999 ± 0.005	1.000 ± 0.004
^{235}U	1.194 ± 0.008	1.195 ± 0.008	1.195 ± 0.006
^{233}U	1.146 ± 0.011	1.142 ± 0.011	1.144 ± 0.008

TABLE 6.4. ^{241}Pu Neutron-detector Efficiency Averaged from All the Standards

S	$\epsilon_n(^{241}\text{Pu})$ Derived from $\epsilon_n(\text{S}) [\times 10^4]$
^{235}U	6.226 ± 0.033
^{233}U	6.294 ± 0.055
^{239}Pu	6.203 ± 0.026
Weighted average	6.220 ± 0.021

Results of other measurements on $\bar{\nu}_p(^{241}\text{Pu})$ are listed in Table 6.5. For each reference, the value of $\bar{\nu}_p(^{241}\text{Pu})$ has been corrected to the standard values of Table 4.2.

TABLE 6.5. Summary of Measurements of $\bar{\nu}_p(^{241}\text{Pu})$

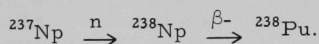
Reference	$\frac{\bar{\nu}_p(^{241}\text{Pu})}{\bar{\nu}_p(^{239}\text{Pu})}$	$\frac{\bar{\nu}_p(^{241}\text{Pu})}{\bar{\nu}_p(^{235}\text{U})}$	$\bar{\nu}_p(^{241}\text{Pu})^a$	Method ^b
Kalashnikova (1956) ³⁷	1.04 ± 0.01	1.24 ± 0.01	2.986 ± 0.030	Comparison of coincidence rates. Ion chamber and BF ₃ counters in paraffin.
Sanders (1956) ⁵¹	1.055 ± 0.050	1.232 ± 0.052	3.015 ± 0.125	Comparison of coincidence rates. Ion chamber and BF ₃ counters in paraffin.
Jaffey (1959) ^{35a}	1.006 ± 0.024	1.208 ± 0.028	2.911 ± 0.067	Comparison of neutron yields of unknown and standards.
de Saussure (1959) ¹⁷	1.053 ± 0.018	1.295 ± 0.019	3.096 ± 0.051	Comparison of coincidence rates. Ion chamber and Hornyak buttons.
Colvin (1965, 1967) ^{12,13}	1.021 ± 0.012	1.212 ± 0.011	2.931 ± 0.027	Comparison of coincidence rates. Ion chamber and BF ₃ counters in graphite (*).
Boldeman (1965, 1967) ^{5,6a}	1.015 ± 0.004	1.220 ± 0.005	2.931 ± 0.010	Comparison of coincidence rates. Ion chamber and organic scintillator (*).
Westcott (1965) ⁶⁰	1.031 ± 0.010	1.224 ± 0.010	2.954 ± 0.023	Review.
Fillmore (1968) ⁷²	1.017 ± 0.003	1.219 ± 0.004	2.933 ± 0.007	Review.
Jaffey (1969)	1.000 ± 0.004	1.195 ± 0.006	2.874 ± 0.015	Present work (*).

^aRecalculated using new σ_F -values⁶⁰ and g-factors.^{42,61} The experiment yielded a $\bar{\nu}$ -value; it has been corrected for delayed neutrons to give $\bar{\nu}_p$.

^bExperiments in which variation of neutron-detection efficiency with neutron spectrum was checked or allowed for are indicated with (*).

6.2. ^{238}Pu

The ^{238}Pu used in the measurement of $\bar{\nu}$ was formed by neutron irradiation of ^{237}Np through the reactions



The interfering ^{239}Pu was also formed through a second-order neutron-capture reaction, and because its thermal fission cross section far exceeds that of ^{238}Pu , it was necessary to keep the ^{239}Pu concentration low. The relatively high capture cross section of ^{238}Pu then required that the ^{237}Np be irradiated with a small total flux-time (nvt).

Mass-spectrometric analysis of the ^{238}Pu sample is shown in Table 6.6.

TABLE 6.6. Isotopic Composition and Fission Properties of ^{238}Pu Sample

	Atom Percent	Half-life (yr) ⁴¹	Spontaneous Fission Half-life (yr) ³²	Specific Activity from Spontaneous Fission (fissions/min/ μg)	Effective Thermal-neutron Fission Cross Section (b)
^{238}Pu	99.663 ± 0.003	86	5×10^{10}	0.068	18.3 ± 0.5^{32}
^{239}Pu	0.310 ± 0.003	24,400	-	-	783.4 ± 4.3^a
^{240}Pu	0.012 ± 0.002	6,580	1.34×10^{11}	0.025	$< 0.005^{32}$
^{241}Pu	< 0.0013	14.0^{48}	-	-	1058 ± 11^a
^{242}Pu	0.014 ± 0.003	379,000	6.5×10^{10}	0.05	$< 0.3^{32}$

^a $\sigma_F(0.0253 \text{ eV})^{60}$ and $g_F^{42,61}$

TABLE 6.7. Measured Neutron Yield Ratios for ^{238}Pu Sample and Standards for Most Extensive Run

	$\bar{c}^* \pm s(\bar{c}^*) [\times 10^3]$
^{239}Pu	2.093 ± 0.006
^{235}U	1.699 ± 0.005
^{233}U	1.773 ± 0.005
^{252}Cf	2.737 ± 0.009
^{238}Pu	2.118 ± 0.021

From Table 6.6, it is seen that spontaneous fission was negligible; this was borne out by experimental measurement with the neutron beam cut off. The values of \bar{c}^* for the most extensive run are given in Table 6.7.

From Table 6.6, the ratio of ^{239}Pu fission rate to ^{238}Pu fission rate in the ^{238}Pu samples was 0.1332 ± 0.0038 . As with the ^{241}Pu sample, the error in the ratio was unimportant, because the difference between $\bar{\nu}_p(^{238}\text{Pu})$ and $\bar{\nu}_p(^{239}\text{Pu})$ is so small. $\epsilon_n(^{238}\text{Pu})$ was taken to be the same as $\epsilon_n(^{239}\text{Pu})$.

Calculated $\bar{\nu}_p$ -ratios for the most extensive run are given in Table 6.8.

For the most extensive run, $\epsilon_n(^{238}\text{Pu})$ -values calculated from the four standards are in Table 6.9.

TABLE 6.8. $\bar{\nu}_p$ -ratios for ^{238}Pu Relative to Standards for Most Extensive Run

S	$\frac{\bar{\nu}_p(^{238}\text{Pu})}{\bar{\nu}_p(\text{S})}$
^{239}Pu	1.014 ± 0.011
^{235}U	1.218 ± 0.014
^{233}U	1.177 ± 0.014
^{252}Cf	0.770 ± 0.009

TABLE 6.9. ^{238}Pu Neutron-detector Efficiency Averaged from All the Standards for Most Extensive Run

S	$\epsilon_n(^{238}\text{Pu})$ Derived from $\epsilon_n(\text{S})$ [$\times 10^4$]
^{239}Pu	7.257 ± 0.028
^{235}U	7.235 ± 0.039
^{233}U	7.268 ± 0.047
^{252}Cf	7.315 ± 0.072
Average	7.270 ± 0.025

Then, after correcting for the ^{239}Pu fission, $\bar{\nu}_p(^{238}\text{Pu}) = 2.918 \pm 0.032$ for the most extensive run.

Some shorter runs yielded results of poorer statistical accuracy. Since the differences from the results of the most extensive run were within the statistical errors, these runs have been included (see Table 6.10), to give average $\bar{\nu}_p$ -ratios and an average value of

$$\bar{\nu}_p(^{238}\text{Pu}) = 2.895 \pm 0.027.$$

TABLE 6.10. ^{238}Pu $\bar{\nu}_p$ -ratios and Average $\bar{\nu}_p$ -values for All the Runs

Run	$\frac{\bar{\nu}_p(^{238}\text{Pu})}{\bar{\nu}_p(^{239}\text{Pu})}$	$\frac{\bar{\nu}_p(^{238}\text{Pu})}{\bar{\nu}_p(^{235}\text{U})}$	$\frac{\bar{\nu}_p(^{238}\text{Pu})}{\bar{\nu}_p(^{233}\text{U})}$	$\frac{\bar{\nu}_p(^{238}\text{Pu})}{\bar{\nu}_p(^{252}\text{Cf})}$	$\bar{\nu}_p(^{238}\text{Pu})$
1	1.014 ± 0.011	1.218 ± 0.014	1.177 ± 0.014	0.770 ± 0.009	2.918 ± 0.032
2	1.034 ± 0.024	1.199 ± 0.031	1.168 ± 0.028	0.783 ± 0.022	2.928 ± 0.072
3	0.964 ± 0.037	1.154 ± 0.040	1.106 ± 0.043	0.727 ± 0.028	2.759 ± 0.104
4	0.977 ± 0.023	1.174 ± 0.028	1.139 ± 0.027	0.749 ± 0.018	2.822 ± 0.067
Weighted Average:	1.008 ± 0.011	1.204 ± 0.012	1.165 ± 0.012	0.765 ± 0.008	2.895 ± 0.027

6.3. ^{241}Am and $^{242\text{m}}\text{Am}$

Pure ^{241}Am was extracted from a plutonium sample containing ^{241}Pu . The plutonium had been previously purified of americium several times, so the sample history would lead to the conclusion that the ^{241}Am samples were probably isotopically pure. This was borne out by the mass-spectrographic analysis (see Table 6.11).

Neutron irradiation of ^{241}Am leads to a metastable excited state as well as the ground state of ^{242}Am . The ground state rapidly decays to ^{242}Cm and ^{242}Pu , but the metastable state ($^{242\text{m}}\text{Am}$) has a relatively long lifetime.

Because of the high fission cross section of $^{242\text{m}}\text{Am}$ and the low capture cross section to the metastable state, the equilibrium concentration of $^{242\text{m}}\text{Am}$ is low. The isotopic composition is shown in Table 6.11.

TABLE 6.11. Isotopic Composition and Fission Properties of Americium Samples

	Atom Percent		Half-life (yr)	Spontaneous Fission Half-life (yr) ³²	Specific Activity from Spontaneous Fission [fissions/min/ μg]	Effective Thermal Fission Cross Section (b)
	^{241}Am Samples	$^{242\text{m}}\text{Am}$ Samples				
^{241}Am	100.0	97.54 \pm 0.01	433 ⁴⁸	2.3 $\times 10^{14}$	1.4 $\times 10^{-5}$	3.1 \pm 0.15 ³²
^{242}Am	<0.003 ^a	1.32 \pm 0.01	152 ⁴¹	9.5 $\times 10^{11}$ ¹¹	0.0035	7300 \pm 330 ¹⁰
^{243}Am	<0.001 ^a	1.14 \pm 0.01	7950 ⁴¹	3.3 $\times 10^{13}$	1 $\times 10^{-4}$	<0.05 ³²

^aLimit of detection.

The table indicates that the spontaneous-fission activity from americium isotopes was negligible. However, $^{242\text{m}}\text{Am}$ decays to the ground state which in turn decays to ^{242}Cm , a nuclide with a relatively short half-life for spontaneous fission. Measurements with the closed shutter indicated that <0.2% of the fission from the $^{242\text{m}}\text{Am}$ sample was spontaneous. This was considered negligible.[†]

Taking $\bar{\nu}_p(^{241}\text{Am}) \cong \bar{\nu}_p(^{242\text{m}}\text{Am}) \cong 3.2$, from (4.31), $\bar{E}(\text{Am})/\bar{E}(^{235}\text{U}) \cong 1.07$. From Fig. 4.1, $\epsilon_n(\text{Am})/\epsilon_n(^{235}\text{U}) = 1.026 \pm 0.007$.

$\bar{\sigma}^*$ -values are given in Table 6.12. Relative $\bar{\nu}_p$ -ratios are in Table 6.13.

TABLE 6.12. Measured Neutron Yield Ratios for Americium and Standard Samples

	$\bar{\sigma}^* \pm s(\bar{\sigma}^*) [\times 10^3]$
^{239}Pu	1.763 \pm 0.006
^{235}U	1.435 \pm 0.004
^{233}U	1.475 \pm 0.004
^{252}Cf	2.284 \pm 0.020
^{241}Am	1.962 \pm 0.020
$^{242\text{m}}\text{Am}$	1.989 \pm 0.008

TABLE 6.13. $\bar{\nu}_p$ -ratios for ^{241}Am and $^{242\text{m}}\text{Am}$ Relative to Standards

S	$\frac{\bar{\nu}_p(^{241}\text{Am})}{\bar{\nu}_p(\text{S})}$	$\frac{\bar{\nu}_p(^{242\text{m}}\text{Am})}{\bar{\nu}_p(\text{S})}$
^{239}Pu	1.112 \pm 0.013	1.127 \pm 0.008
^{235}U	1.332 \pm 0.017	1.351 \pm 0.012
^{233}U	1.310 \pm 0.017	1.329 \pm 0.011
^{252}Cf	0.854 \pm 0.013	0.866 \pm 0.010

$\epsilon_n(\text{Am})$ -values calculated from the four standards are given in Table 6.14. ϵ_n is taken as the same for both americium isotopes. Then,

$$\bar{\nu}_p(^{241}\text{Am}) = 3.219 \pm 0.038,$$

[†]The effect on the calculation of $\bar{\nu}_p(^{242\text{m}}\text{Am})$ is even <0.2%, since the correction is of the order of $0.2\% \times [\bar{\nu}_p(^{242}\text{Cm}) - \bar{\nu}_p(^{242\text{m}}\text{Am})]$.

and, correcting for ^{241}Am fission,[†]

$$\bar{\nu}_p(^{242\text{m}}\text{Am}) = 3.264 \pm 0.024.$$

TABLE 6.14. Americium Neutron-detector Efficiency
Averaged from All the Standards

S	$\epsilon_n(\text{Am})$ Derived from $\epsilon_n(\text{S}) [\times 10^4]$	S	$\epsilon_n(\text{Am})$ Derived from $\epsilon_n(\text{S}) [\times 10^4]$
^{239}Pu	6.119 ± 0.037	^{233}U	6.041 ± 0.048
^{235}U	6.117 ± 0.047	^{252}Cf	6.104 ± 0.072
Average: 6.095 ± 0.035^a			

^aError corrected for correlations.

Results of other measurements on these two nuclides are listed in Table 6.15.

TABLE 6.15. Summary of Measurements of $\bar{\nu}_p(^{241}\text{Am})$ and $\bar{\nu}_p(^{242\text{m}}\text{Am})$

Reference	$\frac{\bar{\nu}_p(\text{Am})}{\bar{\nu}_p(^{235}\text{U})}$	$\frac{\bar{\nu}_p(\text{Am})}{\bar{\nu}_p(^{233}\text{U})}$	$\frac{\bar{\nu}_p(\text{Am})}{\bar{\nu}_p(^{252}\text{Cf})}$	$\bar{\nu}_p(\text{Am})^a$	Method ^b
<u>^{241}Am</u>					
Lebedev (1959) ⁴⁰	1.27 ± 0.01			3.057 ± 0.026	Comparison of coincidence rates. Ion chamber and BF_3 counters in paraffin.
Jaffey (1969)	1.332 ± 0.017	1.310 ± 0.017	0.854 ± 0.013	3.219 ± 0.038	Present work (*).
<u>$^{242\text{m}}\text{Am}$</u>					
Fultz (1966) ²³	1.333 ± 0.066	1.276 ± 0.051	0.857 ± 0.032	3.23 ± 0.12	Comparison of coincidence rates. Spark chamber and BF_3 counters in paraffin (*).
Jaffey (1969)	1.351 ± 0.012	1.329 ± 0.011	0.866 ± 0.010	3.264 ± 0.024	Present work (*).

^aRecalculated, using $\bar{\nu}_p$ -values in Table 4.2.

^bExperiments in which variation of neutron-detection efficiency with neutron spectrum was checked or allowed for are indicated with (*).

6.4. ^{244}Cm

^{244}Cm was present in the samples used for measuring $\bar{\nu}_p(^{243}\text{Cm})$ and $\bar{\nu}_p(^{245}\text{Cm})$. To correct for the spontaneous fission of ^{244}Cm , it was necessary to measure these samples with the beam shutter closed. These measurements, combined with the results (4.20), as in (4.22), yield a value for $\bar{\nu}_p(^{244}\text{Cm})$. The fission rate of ^{244}Cm was quite low in the ^{243}Cm samples, so the statistical accuracy of these runs was limited.

[†] $f(^{241}\text{Am})/f(^{242\text{m}}\text{Am}) = 0.031 \pm 0.002$, from Table 6.11.

For the purpose of using Fig. 4.1, $\bar{\nu}_p(^{244}\text{Cm})$ was taken as ≈ 2.7 . From Eq. (4.31), $\bar{E}(^{244}\text{Cm})/\bar{E}(^{235}\text{U}) \approx 1.026$. The calibration curve (see Fig. 4.1) then gave $\epsilon_n(^{244}\text{Cm})/\epsilon_n(^{235}\text{U}) = 1.021 \pm 0.007$.

$\bar{\epsilon}^*$ -values are shown in Table 6.16.

TABLE 6.16. Measured Neutron Yield Ratios for ^{244}Cm Samples and Standards

Run	$\bar{\epsilon}^* \pm s(\bar{\epsilon}^*) [\times 10^3]$							
	In ^{243}Cm Samples				In ^{245}Cm Samples			
	I	II	III	IV	V	VI	VII	VIII
^{239}Pu	2.742 ± 0.009	2.323 ± 0.007	2.103 ± 0.006	1.893 ± 0.005	2.609 ± 0.006	1.849 ± 0.006	1.897 ± 0.007	1.871 ± 0.016
^{235}U	2.262 ± 0.005	1.887 ± 0.006	1.722 ± 0.008	1.547 ± 0.004	2.132 ± 0.010	1.515 ± 0.004	1.553 ± 0.008	1.502 ± 0.015
^{233}U	2.352 ± 0.007	1.963 ± 0.006	1.776 ± 0.010	1.592 ± 0.005	2.199 ± 0.006	1.572 ± 0.004	1.615 ± 0.006	1.575 ± 0.006
^{252}Cf	3.496 ± 0.016	3.015 ± 0.016						
^{244}Cm	2.469 ± 0.098	2.054 ± 0.079	1.864 ± 0.018	1.763 ± 0.041	2.344 ± 0.018	1.657 ± 0.010	1.687 ± 0.018	1.667 ± 0.028
Ratio of (fission rate, ^{242}Cm) to (fission rate, ^{244}Cm) (calc)	0.027 ± 0.003	0.0053 ± 0.0007			0.0153 ± 0.0006			

A small correction was made for the spontaneous fission of the ^{242}Cm present in the samples. The relative fission rates, calculated from data in Tables 6.20 and 6.24 below, are shown in Table 6.16. The correction, entered as in Eqs. (4.14) and (4.19), involves the value of $\bar{\nu}_p(^{242}\text{Cm})$. This did not have to be known accurately, since the correction was small. Using the ratio $\bar{\nu}_p(^{242}\text{Cm})/\bar{\nu}_p(^{244}\text{Cm}) = 0.933 \pm 0.043^{28}$ and $\bar{\nu}_p(^{244}\text{Cm}) = 2.69$, we have $\bar{\nu}_p(^{242}\text{Cm}) \approx 2.51$.

Calculated $\bar{\nu}_p$ -ratios relative to the standards are shown in Table 6.17.

TABLE 6.17. $\bar{\nu}_p$ -ratios for ^{244}Cm Relative to Standards^a

Run	S			
	^{239}Pu	^{235}U	^{233}U	^{252}Cf
^{243}Cm { I	0.940 \pm 0.037	1.112 \pm 0.045	1.079 \pm 0.044	0.734 \pm 0.029
Samples { II	0.922 \pm 0.036	1.107 \pm 0.044	1.074 \pm 0.042	0.707 \pm 0.028
Average	0.931 \pm 0.026	1.109 \pm 0.032	1.076 \pm 0.031	0.720 \pm 0.020
^{245}Cm { III	0.925 \pm 0.010	1.102 \pm 0.013	1.078 \pm 0.014	
Samples { IV	0.972 \pm 0.022	1.161 \pm 0.028	1.103 \pm 0.027	
{ V	0.937 \pm 0.009	1.119 \pm 0.012	1.095 \pm 0.010	
{ VI	0.935 \pm 0.008	1.113 \pm 0.009	1.083 \pm 0.009	
{ VII	0.928 \pm 0.014	1.103 \pm 0.015	1.072 \pm 0.013	
{ VIII	0.930 \pm 0.018	1.130 \pm 0.023	1.087 \pm 0.020	
Average	0.938 \pm 0.009	1.121 \pm 0.011	1.086 \pm 0.007	
Average of both kinds of samples	0.937 \pm 0.008	1.120 \pm 0.010	1.086 \pm 0.007	0.720 \pm 0.020

^aIn the averaging process, estimating the error of the average includes the fact that each ratio contains the common error in the R-value.

Then, from Eqs. (4.17) and (4.19), we calculate $\bar{\epsilon}_n(^{244}\text{Cm})$ and $\bar{\nu}_p(^{244}\text{Cm})$, as in Table 6.18. The averaged value from the two types of samples is

$$\bar{\nu}_p(^{244}\text{Cm}) = 2.692 \pm 0.024.$$

TABLE 6.18. $\bar{\nu}_p(^{244}\text{Cm})$ -values Averaged from All the Standards

Run	S				$\bar{\epsilon}_n(^{244}\text{Cm}) \left[\times 10^4 \right]$	$\bar{\nu}_p(^{244}\text{Cm})$
	^{239}Pu	$\epsilon_n(^{244}\text{Cm})$ Derived from $\epsilon_n(\text{S})$ ^{235}U	^{233}U	^{252}Cf		
^{243}Cm { I	9.470 ± 0.077	9.595 ± 0.073	9.605 ± 0.077	9.297 ± 0.086	9.492 ± 0.072	2.706 ± 0.109
Samples { II	8.023 ± 0.064	8.004 ± 0.064	8.016 ± 0.064	8.018 ± 0.077	8.015 ± 0.035	2.661 ± 0.104
Average						2.684 ± 0.076
^{245}Cm { I II III IV V VI VII VIII	7.264 ± 0.058	7.304 ± 0.063	7.253 ± 0.068		7.273 ± 0.045	2.663 ± 0.033
	6.538 ± 0.051	6.562 ± 0.051	6.502 ± 0.053		6.534 ± 0.030	2.806 ± 0.068
	9.010 ± 0.073	9.044 ± 0.079	8.981 ± 0.073		9.012 ± 0.044	2.703 ± 0.028
	6.386 ± 0.052	6.426 ± 0.052	6.420 ± 0.052		6.411 ± 0.030	2.686 ± 0.024
	6.551 ± 0.054	6.588 ± 0.059	6.596 ± 0.054		6.578 ± 0.033	2.665 ± 0.034
	6.462 ± 0.073	6.371 ± 0.079	6.432 ± 0.054		6.422 ± 0.040	2.697 ± 0.050
Average						2.693 ± 0.025^a
Average of both kinds of samples						2.692 ± 0.024

^aThe error in the average has been adjusted to take into account the fact that in propagation of errors, each individual $\bar{\nu}_p$ -value contains the same errors in R and $[\epsilon_n(^{244}\text{Cm}) / \epsilon_n(S)]$.

The results of other measurements are listed in Table 6.19.

TABLE 6.19. Summary of $\bar{\nu}_p(^{244}\text{Cm})$ Measurements

Reference	$\bar{\nu}_p(^{244}\text{Cm})$ $\bar{\nu}_p(^{233}\text{U})$	$\bar{\nu}_p(^{244}\text{Cm})$ $\bar{\nu}_p(^{235}\text{U})$	$\bar{\nu}_p(^{244}\text{Cm})$ $\bar{\nu}_p(^{239}\text{Pu})$	$\bar{\nu}_p(^{244}\text{Cm})$ $\bar{\nu}_p(^{252}\text{Cf})$	$\bar{\nu}_p(^{244}\text{Cm})$ $\bar{\nu}_p(^{240}\text{Pu})$	$\bar{\nu}_p(^{244}\text{Cm})^a$	Method ^b
Hicks (1955) ²⁷				0.7407 ± 0.055		2.788 ± 0.021	Comparison of coincidence rates. Ion chamber and cadmium-loaded scintillator.
Higgins (1955) ²⁹						2.60 ± 0.11^c	Comparison of activation of Mn in MnSO_4 bath. Relative to calibrated Po-Be sources.
Diven (1956) ^{20d}	1.087 ± 0.035 $[2.694 \pm 0.087]$	1.138 ± 0.028 $[2.739 \pm 0.068]$	0.922 ± 0.031 $[2.659 \pm 0.090]$	0.726 ± 0.021 $[2.732 \pm 0.079]$	1.245 ± 0.036 $[2.679 \pm 0.078]$	2.700 ± 0.057	Comparison of coincidence rates. Fragment counter and cadmium-loaded scintillator.
Hicks (1956) ^{28d}				0.743 ± 0.033 $[2.797 \pm 0.124]$	1.258 ± 0.047 $[2.707 \pm 0.102]$	2.752 ± 0.102	As in Ref. 27.
Crane (1956) ¹⁶				0.741 ± 0.016 $[2.789 \pm 0.062]$	1.246 ± 0.046 $[2.681 \pm 0.098]$	2.753 ± 0.055	Comparison of coincidence rates. Ion chamber and Li(Eu) neutron detector.
Bol'shov (1964) ^{7d}					1.250 ± 0.018 $[2.690 \pm 0.040]$	2.690 ± 0.040	Comparison of coincidence rates. Ion chamber and BF ₃ counters in paraffin.
Jaffey (1969)	1.086 ± 0.007	1.120 ± 0.010	0.937 ± 0.008	0.720 ± 0.020		2.692 ± 0.024	Present work (*).

^aRecalculated, using $\bar{\nu}_p$ -values in Table 4.2 or relative to $\bar{\nu}_p(^{240}\text{Pu})$.

^bExperiments in which variation of neutron detection efficiency with neutron spectrum was checked or allowed for are indicated with (*).

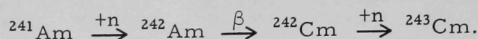
^cTotal neutron yield measured ($\bar{\nu}$).

^dThe quantities in [] are values of $\bar{\nu}_p(^{244}\text{Cm})$ calculated using standard values of Table 4.2; $\bar{\nu}_p(^{240}\text{Pu})$ is taken as 2.152 ± 0.007 , averaged from:

Diven (1961) ²¹	$\frac{\bar{\nu}_p(^{240}\text{Pu})}{\bar{\nu}_p(^{235}\text{U})} = 0.903 \pm 0.0074 \rightarrow \bar{\nu}_p(^{240}\text{Pu}) = 2.174 \pm 0.018$
Moat (1961) ⁴⁷	$\frac{\bar{\nu}_p(^{240}\text{Pu})}{\bar{\nu}_p(^{252}\text{Cf})} = 0.576 \pm 0.006 \rightarrow \bar{\nu}_p(^{240}\text{Pu}) = 2.168 \pm 0.024$
Asplund-Nilsson (1963) ¹	$\frac{\bar{\nu}_p(^{240}\text{Pu})}{\bar{\nu}_p(^{252}\text{Cf})} = 0.5668 \pm 0.0037 \rightarrow \bar{\nu}_p(^{240}\text{Pu}) = 2.134 \pm 0.017$
Colvin (1965) ¹²	$\frac{\bar{\nu}_p(^{240}\text{Pu})}{\bar{\nu}_p(^{235}\text{U})} = 0.888 \pm 0.005 \rightarrow \bar{\nu}_p(^{240}\text{Pu}) = 2.137 \pm 0.013$
Baron (1967) ³	$\frac{\bar{\nu}_p(^{240}\text{Pu})}{\bar{\nu}_p(^{252}\text{Cf})} = 0.5693 \pm 0.0039 \rightarrow \bar{\nu}_p(^{240}\text{Pu}) = 2.143 \pm 0.017$
Boldeman (1968) ^{6b}	$\frac{\bar{\nu}_p(^{240}\text{Pu})}{\bar{\nu}_p(^{252}\text{Cf})} = 0.5729 \pm 0.0024 \rightarrow \bar{\nu}_p(^{240}\text{Pu}) = 2.156 \pm 0.013.$

6.5. ^{243}Cm

^{243}Cm can be formed by successive neutron captures and β decays with ^{241}Am as starting material:



After the americium and plutonium components are separated from such an irradiation, the curium fraction contains a mixture of ^{242}Cm and ^{243}Cm , together with ^{244}Cm , ^{245}Cm , and ^{246}Cm . The last three isotopes are formed through successive neutron captures by ^{243}Cm . Interference from the relatively high concentration of ^{244}Cm is not serious, since the effect of its spontaneous fission can be corrected. However, the pulse-pileup problem due to the very intense α activity from the short-lived ^{242}Cm made it difficult to use a freshly irradiated sample. We were fortunate in being able to borrow a sample* which had decayed $3\frac{1}{2}$ yr after irradiation, with an attendant 230-fold decrease in the ^{242}Cm component. The mass-spectrometric analysis of the sample at the time of the $\bar{\nu}$ -measurement is shown in Table 6.20. Two $\bar{\nu}$ -measurements were made about a year apart, and the mass analysis (II) was actually made at the time of the second measurement. Compositions at the times of the two $\bar{\nu}$ -measurements are shown as I and II; decay corrections were made from the known half-lives.

TABLE 6.20. Isotopic Composition and Fission Properties of ^{243}Cm Samples

	Atom Percent		Half-life (yr) ⁴¹	Spontaneous Fission Half-life (yr) ³²	Specific Activity from Spontaneous Fission [fissions/min/ μg]	Fission Cross Sections (b)
	I	II				
^{242}Cm	0.81 ± 0.09	0.161 ± 0.028	0.446	7.2×10^6	459	
^{243}Cm	40.2 ± 0.4	40.9 ± 0.4	32	-	-	690^{32}
^{244}Cm	58.4 ± 0.6	58.3 ± 0.6	18.10^4	$(1.346 \pm 0.006) \times 10^7$	241.5 ± 1.1	
^{245}Cm	0.66 ± 0.08	0.69 ± 0.08	9300	-	-	2040^{19}
^{246}Cm	0.0052 ± 0.0007	0.0054 ± 0.0007	5500	1.66×10^7	196	

From Table 6.20, we note that $[\text{fission rate } ^{243}\text{Cm}]/[\text{fission rate } ^{245}\text{Cm}] \approx 20$. Since $\bar{\nu}_p(^{245}\text{Cm})$ is fairly close to $\bar{\nu}_p(^{243}\text{Cm})$, an adequate correction can be made even if $\bar{\nu}_p(^{245}\text{Cm})$ is not known accurately. For this correction we use the value $\bar{\nu}_p(^{245}\text{Cm}) \approx 3.80$. The fission rate of ^{245}Cm relative to ^{243}Cm was calculated from the composition and fission cross sections of Table 6.20. Calculation similarly yielded the relative fission rates of ^{242}Cm and ^{244}Cm . The ratio of the measured fission rates of ^{244}Cm relative to the total fission rate is given in Table 6.21.

The relations (4.18) or (4.26) may be used here, and give about the same result. We shall use (4.18) for these data, with the value

*We are indebted for the source of this sample to E. K. Hulet, Lawrence Radiation Laboratory, University of California, Livermore.

$\bar{\nu}_p(^{244}\text{Cm}) = 2.692 \pm 0.024$, from the previous section. Experimental results are shown in Table 6.21.

TABLE 6.21. Measured Neutron Yield Ratios
for ^{243}Cm Samples and Standards

Sample	$\bar{\epsilon}^* \pm s(\bar{\epsilon}^*) [\times 10^3]$	
	I	II
^{239}Pu	2.742 ± 0.009	2.323 ± 0.007
^{235}U	2.262 ± 0.005	1.887 ± 0.006
^{233}U	2.352 ± 0.007	1.963 ± 0.006
^{252}Cf	3.496 ± 0.016	3.015 ± 0.016
Cm	3.171 ± 0.045	2.661 ± 0.017
$\frac{\text{Fission rate, } ^{245}\text{Cm}}{\text{Fission rate, } ^{243}\text{Cm}}$ (calculated)	0.049 ± 0.006	0.050 ± 0.006
$\frac{\text{Fission rate, } ^{244}\text{Cm}}{\text{Total fission rate}}$ (measured)	0.1804 ± 0.0023	0.1648 ± 0.0065
$\frac{\text{Fission rate, } ^{242}\text{Cm}}{\text{Fission rate, } ^{244}\text{Cm}}$ (calculated)	0.0265 ± 0.0029	0.0053 ± 0.0007

For use of Fig. 4.1, $\bar{\nu}_p(^{243}\text{Cm})$ was taken as ≈ 3.4 . From Eq. (4.31), $\bar{E}(^{243}\text{Cm})/\bar{E}(^{235}\text{U}) \approx 1.074$. The curve gives $\epsilon_n(^{243}\text{Cm})/\epsilon_n(^{235}\text{U}) = 1.025 \pm 0.007$. Similar calculations give $\epsilon_n(^{242}\text{Cm})/\epsilon_n(^{235}\text{U}) = 1.011$, $\epsilon_n(^{244}\text{Cm})/\epsilon_n(^{235}\text{U}) = 1.021$, $\epsilon_n(^{245}\text{Cm})/\epsilon_n(^{235}\text{U}) = 1.020$.

Ratios of $\bar{\nu}_p(^{243}\text{Cm})$ to the standard values are shown in Table 6.22.

TABLE 6.22. $\bar{\nu}_p$ -ratios for ^{243}Cm Relative to Standards

	S			
	^{239}Pu	^{235}U	^{233}U	^{252}Cf
I	1.199 ± 0.027	1.418 ± 0.032	1.376 ± 0.031	0.943 ± 0.021
II	1.182 ± 0.023	1.420 ± 0.027	1.377 ± 0.026	0.905 ± 0.018
Average	1.189 ± 0.018	1.419 ± 0.021	1.377 ± 0.020	0.921 ± 0.014

From Eqs. (4.17) and (4.19), we calculate $\bar{\epsilon}_n(^{243}\text{Cm})$ and $\bar{\nu}_p(^{243}\text{Cm})$, as in Table 6.23. The result, averaged over the two samples, was

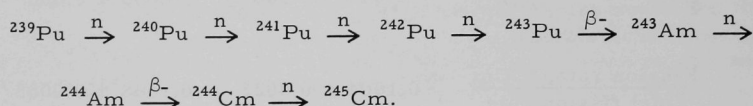
$$\bar{\nu}_p(^{243}\text{Cm}) = 3.430 \pm 0.047.$$

TABLE 6.23. $\bar{\nu}_p(^{243}\text{Cm})$ -values Averaged from All the Standards

	S				$\bar{\epsilon}_n(^{243}\text{Cm})$	$\bar{\nu}_p(^{243}\text{Cm})$
	$\epsilon_n(^{243}\text{Cm})$ Derived from $\epsilon_n(S) \left[\times 10^4 \right]$					
	^{239}Pu	^{235}U	^{233}U	^{252}Cf		
I	9.508 ± 0.077	9.632 ± 0.074	9.643 ± 0.078	9.328 ± 0.084	9.528 ± 0.073	3.460 ± 0.078
II	8.055 ± 0.064	8.036 ± 0.064	8.049 ± 0.064	8.050 ± 0.074	8.048 ± 0.032	3.412 ± 0.059
Average						3.430 ± 0.047

6.6. ^{245}Cm

A ^{245}Cm sample was formed by a long irradiation (of high nvt) of ^{239}Pu in which neutron captures and β decays occurred:



The $^{245}\text{Cm}/^{244}\text{Cm}$ ratio was an equilibrium value and small, because of the very large difference in total cross sections. ^{241}Am derived from ^{241}Pu β decay also gave rise to some lower-mass curium isotopes as in the formation of the ^{243}Cm sample (see Sect. 6.5). Higher-mass curium isotopes were formed through further neutron capture by ^{245}Cm .

A mass-spectrographic analysis is shown in Table 6.24.

TABLE 6.24. Isotopic Composition and Fission Properties of ^{245}Cm Sample

	Atom Percent	Half-life (yr) ⁴¹	Spontaneous Fission Half-life (yr) ³²	Specific Activity from Spontaneous Fission [fissions/min/ μg]	Fission Cross Section (b)
^{242}Cm	0.76 ± 0.03	0.446	7.2×10^6	459	-
^{243}Cm	0.053 ± 0.005	32	-	-	690^{32}
^{244}Cm	96.0 ± 0.1	18.10^4	$(1.346 \pm 0.006) \times 10^7$	241.5 ± 1.1	-
^{245}Cm	1.04 ± 0.02	9300	-	-	2040^{19}
^{246}Cm	2.10 ± 0.1	5500	1.66×10^7	196	-
^{247}Cm	0.024 ± 0.008	1.6×10^7	-	-	108^{19}
^{248}Cm	0.008 ± 0.003	4.7×10^5	4.6×10^6	702	-

Corrections were made for the effects of the interfering isotopes ^{242}Cm , ^{243}Cm , and ^{244}Cm . The fission rate of ^{247}Cm was, from Table 6.24, about 0.1% that of ^{245}Cm and is neglected here.*

*An impurity whose relative fission rate is 0.1% changes the calculated $\bar{\nu}_p$ value by <0.1%, because the correction depends upon the fractional difference in $\bar{\nu}_p$ values.

Experimental measurements are shown in Table 6.25. The value of $f(^{244}\text{Cm})$ depended upon the neutron flux at the time of the run; in eight experiments, it varied from 0.433 to 0.705. From the table, we see that $[\text{fission rate } ^{243}\text{Cm}]/[\text{fission rate } ^{245}\text{Cm}] = 0.0172 \pm 0.0017$; the ^{243}Cm correction is a small one; however, the correction for ^{244}Cm is much larger and is considerably more important than in the measurement made of $\bar{\nu}_p(^{243}\text{Cm})$.

TABLE 6.25. Measured Neutron Yield Ratios for ^{245}Cm Sample and Standards

Run	$\bar{C}^* + s(\bar{C}^*) [\times 10^3]$				Ratio of [Fission rate, ^{244}Cm] to [Total fission rate (measured)]	Ratio of [Fission rate, ^{243}Cm] to [Fission rate, ^{245}Cm] (calc.)	Ratio of [Fission rate, ^{242}Cm] to [Fission rate, ^{244}Cm] (calc.)
	^{239}Pu	^{235}U	^{233}U	Cm			
I	1.999 ± 0.009	1.630 ± 0.018	1.683 ± 0.013	2.277 ± 0.014	0.4333 ± 0.0034	0.0172 ± 0.0017	0.0153 ± 0.0006
IIA ^a	2.103 ± 0.006	1.722 ± 0.008	1.776 ± 0.010	2.424 ± 0.026	0.4329 ± 0.0013	↓	↓
IIB				2.199 ± 0.020	0.686 ± 0.011		
III	1.893 ± 0.005	1.547 ± 0.004	1.592 ± 0.005	2.000 ± 0.013	0.6900 ± 0.0030		
IV	2.066 ± 0.016	1.677 ± 0.018	1.755 ± 0.013	2.168 ± 0.018	0.6809 ± 0.0027		
V	2.609 ± 0.006	2.132 ± 0.010	2.199 ± 0.006	2.775 ± 0.029	0.6740 ± 0.0032		
VI	1.849 ± 0.006	1.515 ± 0.004	1.572 ± 0.004	1.966 ± 0.043	0.6708 ± 0.0019		
VII	1.897 ± 0.007	1.553 ± 0.008	1.615 ± 0.006	2.026 ± 0.018	0.5889 ± 0.0099		
VIII	1.871 ± 0.016	1.502 ± 0.015	1.575 ± 0.006	1.924 ± 0.015	0.7055 ± 0.0028		

^aThe flux level dropped during the run. \bar{C} -values for the standards were not affected, but the relative \bar{C} -value for the curium samples did change because of the shift in relative fissions of ^{245}Cm and ^{244}Cm . $\bar{\nu}_p$ -results for both measurements are averaged.

Ratios of $\bar{\nu}_p(^{245}\text{Cm})$ to the standard values are shown in Table 6.26. The ϵ_n -values are those used in Sect. 6.5.

TABLE 6.26. $\bar{\nu}_p$ -ratios for ^{245}Cm Relative to Standards

Run	S		
	^{239}Pu	^{235}U	^{233}U
I	1.313 ± 0.027	1.570 ± 0.041	1.539 ± 0.037
II	1.335 ± 0.028	1.585 ± 0.032	1.559 ± 0.033
III	1.366 ± 0.055	1.621 ± 0.066	1.614 ± 0.065
IV	1.328 ± 0.064	1.605 ± 0.082	1.529 ± 0.079
V	1.366 ± 0.065	1.622 ± 0.080	1.604 ± 0.077
VI	1.361 ± 0.081	1.605 ± 0.099	1.563 ± 0.097
VII	1.283 ± 0.093	1.520 ± 0.111	1.473 ± 0.107
VIII	1.288 ± 0.072	1.607 ± 0.090	1.520 ± 0.078
Average	1.328 ± 0.013	1.591 ± 0.016	1.553 ± 0.016

$\bar{\epsilon}_n(^{245}\text{Cm})$ and $\bar{\nu}_p(^{245}\text{Cm})$ are calculated as before, with results as in Table 6.27. The averaged result is

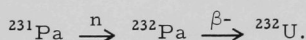
$$\bar{\nu}_p(^{245}\text{Cm}) = 3.832 \pm 0.034.$$

TABLE 6.27. $\bar{\nu}_p(^{245}\text{Cm})$ -values Averaged from All the Standards

Run	S $\epsilon_n(^{245}\text{Cm})$ Derived from $\epsilon_n(\text{S}) [\times 10^4]$			$\bar{\epsilon}_n(^{245}\text{Cm})$	$\bar{\nu}_p(^{245}\text{Cm})$
	^{239}Pu	^{235}U	^{233}U		
I	6.897 ± 0.060	6.907 ± 0.091	6.866 ± 0.079	6.890 ± 0.044	3.793 ± 0.072
II	7.256 ± 0.058	7.297 ± 0.063	7.245 ± 0.057	7.266 ± 0.034	3.842 ± 0.072
III	6.532 ± 0.051	6.556 ± 0.051	6.495 ± 0.053	6.528 ± 0.030	3.945 ± 0.146
IV	7.129 ± 0.076	7.107 ± 0.092	7.160 ± 0.076	7.132 ± 0.047	3.826 ± 0.157
V	9.002 ± 0.070	9.035 ± 0.079	8.971 ± 0.072	9.003 ± 0.043	3.938 ± 0.180
VI	6.380 ± 0.051	6.420 ± 0.051	6.413 ± 0.051	6.404 ± 0.029	3.887 ± 0.234
VII	6.546 ± 0.054	6.581 ± 0.059	6.588 ± 0.055	6.572 ± 0.003	3.669 ± 0.262
VIII	6.456 ± 0.073	6.365 ± 0.078	6.425 ± 0.054	6.415 ± 0.040	3.782 ± 0.184
Average					3.832 ± 0.034

6.7. ^{232}U

^{232}U was formed by neutron irradiation of ^{231}Pa :



Since a second-order neutron capture yields the highly fissionable ^{233}U , the total irradiation (nvt) was limited to keep such capture low. The ^{232}U yield per milligram of ^{231}Pa was correspondingly low, and this may explain the presence of ^{235}U and ^{238}U , which may have been present in low concentration in the difficult-to-totally-purify ^{231}Pa source material. The isotopic composition is shown in Table 6.28.

TABLE 6.28. Isotopic Composition and Fission Properties of ^{232}U Sample

	Atom Percent	Half-life (yr) ⁴¹	Spontaneous Fission Half-life (yr) ³²	Specific Activity from Spontaneous Fission (fissions/min/ μg)	Effective Thermal Cross Section (b)
^{232}U	99.213 ± 0.009	72	8×10^{13}	4×10^{-5}	78 ± 4^{55}
^{233}U	0.195 ± 0.004	1.62×10^5			525^{55}
^{235}U	0.078 ± 0.004	7.1×10^8	1.8×10^{17}	2×10^{-8}	557^{55}
^{238}U	0.514 ± 0.007	4.51×10^9	1×10^{16}	3×10^{-7}	$<0.5^{32}$

Experimental results are shown in Table 6.29. We consider the measurements with this nuclide to be less satisfactory than the previous measurements, because the neutron detector showed greater tendency to drift. We used only the data gathered during periods of modest drift, and there was no external evidence of difficulty during these periods. We have made no allowance in the error calculation for the possibility of detector drifts not accounted for. Unfortunately, the ^{232}U measurement could not be repeated, because of termination of the experiment.

TABLE 6.29. Measured Neutron Yield Ratios
for ^{232}U Sample and Standards

Sample	$\bar{\epsilon}^* \pm s(\bar{\epsilon}^*) [\times 10^3]$
^{235}U	1.774 ± 0.008
^{233}U	1.859 ± 0.013
^{232}U	2.371 ± 0.042
$\frac{\text{Fission rate, } ^{235}\text{U}}{\text{Fission rate, } ^{232}\text{U}}$ (calc) ^a	0.0058 ± 0.0003
$\frac{\text{Fission rate, } ^{233}\text{U}}{\text{Fission rate, } ^{232}\text{U}}$ (calc) ^a	0.0132 ± 0.0003

^aRelative fission rates calculated from
Table 6.28.

With a preliminary estimate $\bar{\nu}_p(^{232}\text{U}) \cong 3.1$ and $\bar{E}(^{232}\text{U})/\bar{E}(^{235}\text{U}) = 1.060$; then from Fig. 4.1, $\epsilon_n(^{232}\text{U})/\epsilon_n(^{235}\text{U}) = 1.026 \pm 0.007$. Relative $\bar{\nu}_p$ -ratios are in Table 6.30.

$\epsilon_n(^{232}\text{U})$ -values derived from the two standards are given in Table 6.31.

TABLE 6.30. $\bar{\nu}_p$ -ratios
for ^{232}U Relative
to Standards

S	$\frac{\bar{\nu}_p(^{232}\text{U})}{\bar{\nu}_p(S)}$
^{235}U	1.308 ± 0.026
^{233}U	1.260 ± 0.026

TABLE 6.31. ^{232}U Neutron-
detection Efficiency Averaged
from All the Standards

S	$\epsilon_n(^{232}\text{U})$ Derived from $\epsilon_n(S) [\times 10^4]$
^{235}U	7.562 ± 0.065
^{233}U	7.630 ± 0.078
Average	7.596 ± 0.050

Correcting for ^{235}U and ^{233}U fission in the ^{232}U -sample with Eq. (4.18), we obtain

$$\bar{\nu}_p(^{232}\text{U}) = 3.130 \pm 0.060.$$

7. DISCUSSION

Fission theory is not well enough developed to allow prediction of $\bar{\nu}_p$ -values. The fission energy E_F arises from the difference in mass of the fissioning nucleus and fission fragments, and also from the energy added by the incoming particle. Most of E_F goes into the kinetic energy E_K of the fission fragments. The residual excitation energy $E_X = E_F - E_K$ is a relatively small difference between two large numbers. Hence, even when E_F and E_K are predictable, they must be known very accurately for E_X to be known even moderately well. A further complication is that E_X is shared between neutron and γ -ray emission in proportions that are not understood theoretically, so that $E_X = E_n + E_\gamma$, but E_n is not predictable even when E_X is known.

In view of the difficulty in calculating $\bar{\nu}_p$ from first principles, another approach has been to use theory only to provide a qualitative guide for developing interpolation relations. If we assume that the factors governing the values of E_F , E_K , and E_γ/E_n vary smoothly with Z and A , we may form an interpolation formula for $\bar{\nu}_p$ with adjustable constants. These constants may be least-squares fitted through the use of some measured $\bar{\nu}_p$ -values. Theory enters only qualitatively, by suggesting the most suitable form for such a relation.

Since nuclear masses vary smoothly over the small ranges $90 \leq Z \leq 100$ and $140 \leq N \leq 152$, it has been considered reasonable²⁴ to take $\bar{\nu}_p$ for thermal-neutron fission as approximately a linear function of A and Z , with a minor correction for odd-even effects.* The coefficients were evaluated by fitting the linear relation to the experimental values: ²²⁹Th, 2.09; ²³³U, 2.50; ²³⁵U, 2.43; ²³⁹Pu, 2.89; ²⁴¹Pu, 2.95; ²⁴¹Am, 3.09. The resulting equation was then

$$\bar{\nu}_p = 0.1894 Z + 0.007 A - 16.60 + 0.09 \zeta. \quad (7.1)$$

For a target nucleus with odd N and odd Z we have $\zeta = +1$; $\zeta = -1$ for even N and even Z ; $\zeta = 0$ for odd A .

*Our measurements suggest a change in an interpretation derived from the results calculated in Ref. 24. With $\bar{\nu}_p(^{243}\text{Cm})$ calculated from Eq. (7.1), the difference $\bar{\nu}_p(^{243}\text{Cm} + n) - \bar{\nu}_p(^{244}\text{Cm}, \text{spont.}) = 0.53 \pm 0.12$ was there estimated. Since the same nucleus was fissioning, the difference was due to the added neutron binding energy B_n . However, from the known B_n -value, $\Delta\bar{\nu}_p$ would be predicted to be 0.86 ± 0.08 ; the difference between 0.53 and 0.86 was interpreted as due to an increase in \bar{E}_K in thermal-neutron fission relative to spontaneous fission, with $\Delta\bar{E}_K = 2.5 \pm 1.1$ MeV. With our measured values (see Tables 6.18 and 6.23), we find the difference $\bar{\nu}_p(^{243}\text{Cm} + n) - \bar{\nu}_p(^{244}\text{Cm}, \text{spont.}) = 0.74 \pm 0.05$. The distinction between this value and the calculated value 0.86 ± 0.08 is not statistically significant, so the data are consistent with $\Delta\bar{E}_K = 0$.

With the same nuclides, but with values corrected to the standard values in Table 4.2 [^{229}Th , 2.08; ^{233}U , 2.478; ^{235}U , 2.407; ^{239}Pu , 2.884; ^{241}Pu , 2.933; ^{241}Am , 3.057], a least-squares fit gave

$$\bar{\nu}_p = 0.1909 Z + 0.0088 A - 16.34 + 0.09 \zeta. \quad (7.2)$$

Our experimental values are compared to values predicted from Eq. (7.2) in Table 7.1. On the whole, the experimental values agree qualitatively with Eq. (7.2), in that $\bar{\nu}_p$ changes much more with $\Delta Z = 1$ than with $\Delta A = 1$, and usually $\Delta\bar{\nu}_p$ is positive for $\Delta A > 0$. Quantitative agreement is less good, implying that coefficients which fit best in one (Z, A) range may not apply as well when the range is expanded.

TABLE 7.1. Comparison of Experimental $\bar{\nu}_p$ -values with Semitheoretically Derived Relations^{a,b}

Nuclide	$\bar{\nu}_p$ (Expt)	$\bar{\nu}_p$, Calc from (Z, A) Expansion			$\bar{\nu}_p$, Calc from Z^2/A Expansion	
		From Eq. (7.2)	From Eq. (7.3)	From Eq. (7.4)	From Ref. 50b	Renormalized ^c
^{229}Th	2.080 ± 0.020	2.059 (-0.021)	2.604 (-0.015)	1.977 (-0.103)	2.172 (+0.092)	2.156 (+0.076)
^{232}U	3.130 ± 0.060^a	2.359 (-0.771)	2.514 (-0.616)	2.372 (-0.758)	2.380 (-0.750)	2.345 (-0.785)
^{233}U	2.478 ± 0.007	2.458 (-0.020)	2.568 (+0.090)	2.463 (-0.014)	2.394 (-0.084)	2.376 (-0.102)
^{235}U	2.407 ± 0.005	2.476 (+0.069)	2.495 (+0.088)	2.465 (+0.058)	2.425 (+0.018)	2.407 (0.000)
^{238}Pu	2.895 ± 0.027^a	2.776 (-0.119)	2.945 (+0.050)	2.860 (-0.035)	2.874 (-0.021)	2.853 (-0.042)
^{239}Pu	2.884 ± 0.007	2.875 (-0.009)	2.998 (+0.114)	2.951 (+0.067)	2.896 (+0.012)	2.875 (-0.009)
^{241}Pu	2.874 ± 0.015^a	2.893 (+0.019)	2.926 (+0.052)	2.953 (+0.079)	2.941 (+0.067)	2.919 (+0.045)
^{241}Am	3.219 ± 0.038^a	3.075 (-0.144)	3.250 (+0.031)	3.194 (-0.024)	3.181 (-0.038)	3.157 (-0.062)
^{242m}Am	3.264 ± 0.024^a	3.174 (-0.090)	3.304 (+0.040)	3.285 (+0.021)	3.221 (-0.043)	3.197 (-0.067)
^{243}Cm	3.430 ± 0.047^a	3.274 (-0.156)	3.502 (+0.072)	3.437 (+0.007)	3.501 (+0.071)	3.475 (+0.045)
^{245}Cm	3.832 ± 0.034^a	3.292 (-0.540)	3.429 (-0.403)	3.439 (-0.392)	3.524 (-0.308)	3.498 (-0.334)

^aNumbers in parentheses are $\Delta = \bar{\nu}_p(\text{calc}) - \bar{\nu}_p(\text{expt})$.

^bMeasurements reported in this paper are indicated with (*).

^cRenormalized to $\bar{\nu}_p(^{235}\text{U}) = 2.407$.

We have recalculated Eq. (7.2) including all the values in Tables 6.5, 6.10, 6.15, 6.23, and 6.27, and in Sect. 6.7, with the result

$$\bar{\nu}_p = 0.2881 Z - 0.0363 A - 18.80 + 0.09 \zeta. \quad (7.3)$$

The negative coefficient of A is generated by the large $\bar{\nu}_p$ -value of ^{232}U . If the ^{232}U result is omitted, the least-squares fit gives

$$\bar{\nu}_p = 0.2422 Z + 0.00089 A - 19.95 + 0.09 \zeta. \quad (7.4)$$

Table 7.1 also compares the experimental measurements with Eqs. (7.3) and (7.4). The ^{232}U result does not agree with the very small and positive ΔA -effect predicted by Eqs. (7.1), (7.2), or (7.4). Kuzminov and Smirenkin³⁹ note the possibility that shell effects in the fission fragments may make $\bar{\nu}_p$ increase with decreasing A, and suggest this to be the case for the light uranium isotopes.

In an alternative empirical systematization,^{50a} $\bar{\nu}_p$ is expressed as a polynomial in the fissility parameter Z^2/A , through successive least-squares-fitted polynomial expansions: $\bar{\nu}_p = f(\bar{E}_K)$, $\bar{E}_K = g(E_t)$, and $E_t = h(Z^2/A)$, with E_t = fission threshold energy. Some predicted values are listed in Table 7.1. On the whole, this is a more successful approach.

ACKNOWLEDGMENTS

We wish to acknowledge our appreciation and indebtedness: to Albert Hirsch, for early experiments in developing apparatus and for preliminary measurements with ^{241}Pu ; to Ruth Sjoblom, for preparation of most of the samples; to Lee Harkness, for mass-spectrometric analyses of the samples; to Robert Scott, who aided in the long and tedious gathering of counts; to E. K. Hulet (Livermore) for the use of a ^{243}Cm sample; and to the CP-5 operators, who aided in the initial stages of setting up the experiment, and who were effective in keeping the neutrons coming.

REFERENCES

1. I. Asplund-Nilsson, H. Condé, and N. Starfelt, *Average Number of Prompt Neutrons Emitted in the Spontaneous Fission of ^{238}U and ^{240}Pu* , Nucl. Sci. Eng. 15, 213-216 (1963).
2. E. Barnard, A. T. G. Ferguson, W. R. McMurray, and I. J. van Heerden, *Time-of-flight Measurements of Neutron Spectra from the Fission of ^{235}U , ^{238}U and ^{239}Pu* , Nucl. Phys. 71, 228-240 (1965).
3. E. Baron, J. Frehaut, F. Ouvry, and M. Soleilhac, *Neutrons Prompts de Fission-Mesure de $\bar{\nu}$ et des Probabilités $P(\nu)$ d'Emission de ν Neutrons*, Proc. Conf. Nuclear Data for Reactors, Vol. II, IAEA (1967), pp. 57-66.
4. W. C. Bentley, *Alpha Half-life of ^{244}Cm* , J. Inorg. Nucl. Chem. 30, 2007-2009 (1968).
5. J. W. Boldeman, *A Liquid Scintillator Experiment for Measuring $\bar{\nu}$ for ^{241}Pu* , Proc. Symp. Phys. and Chem. Fission, Vol. II, IAEA (1965), pp. 103-109.
- 6a. J. W. Boldeman and A. W. Dalton, *Prompt $\bar{\nu}$ Measurements for Thermal Neutron Fission*, Australian Atomic Energy Commission Report E-172 (March 1967).
- 6b. J. W. Boldeman, *Prompt $\bar{\nu}$ Measurements for the Spontaneous Fission of ^{240}Pu and ^{242}Pu* , J. Nucl. Energy 22, 63-72 (1968).
7. V. I. Bol'shov, L. I. Prokhorova, V. N. Okolovich, and G. N. Smirenkin, *Some Data on the Spontaneous Fission of ^{244}Cm* , Sovt. Atomic Energy 17, 715-721 (1964); translation from Atomnaya Energiia 17, 28-34 (1964).
8. T. W. Bonner, *Measurements of Neutron Spectra from Fission*, Nucl. Phys. 23, 116-121 (1961).
9. H. R. Bowman, S. G. Thompson, J. C. D. Milton, and W. J. Swiatecki, *Velocity and Angular Distributions of Prompt Neutrons from Spontaneous Fission of ^{252}Cf* , Phys. Rev. 126, 2120-2136 (1962).
10. C. D. Bowman, G. F. Auchampaugh, S. C. Fultz, and R. W. Hoff, *Neutron-induced Cross-section of ^{242m}Am* , Phys. Rev. 166, 1219-1226 (1968).
11. J. T. Caldwell, S. C. Fultz, and C. D. Bowman, *Spontaneous Fission Half-life of ^{242m}Am* , Phys. Rev. 155, 1309-1313 (1967).
12. D. W. Colvin and M. G. Sowerby, *Boron Pile $\bar{\nu}$ Measurements*, Proc Symp. on Phys. and Chem. of Fission, Vol. II, IAEA, Vienna (1965), pp. 25-37.
13. D. W. Colvin, M. G. Sowerby, and R. I. MacDonald, *Confirmatory Experimental Data on the Harwell Boron Pile $\bar{\nu}$ Values*, Proc. Conf. on Nucl. Data for Reactors, Vol. I, IAEA, Vienna (1967), pp. 307-319.
14. H. Condé, *Average Number of Neutrons from the Fission of ^{235}U* , Ark. f. Fysik 29, 293-299 (1965).
15. H. Condé, and G. During, *Fission Neutron Spectra. II. Fission-neutron Spectra of ^{235}U , ^{239}Pu , ^{252}Cf* , Ark. f. Fysik 29, 313-319 (1965).
16. W. W. T. Crane, G. H. Higgins, and H. R. Bowman, *Average Number of Neutrons per Fission for Several Heavy Element Nuclides*, Phys. Rev. 101, 1804-1805 (1956).

17. G. de Saussure and E. G. Silver, *Comparison of the Average Number of Prompt Neutrons Emitted in the Fission of ^{233}U , ^{235}U , ^{239}Pu and ^{241}Pu* , Nucl. Sci. and Eng. 5, 49-54 (1959).
18. A. DeVolpi and K. G. Porges, *Direct and Absolute Measurements of Average Fission Neutron Yield from Uranium-235 and Californium-252*, Proc. Conf. on Nucl. Data for Reactors, Vol. I, IAEA, Vienna (1967), pp. 297-306; ANL-7210 (Dec 1966), pp. 21-23.
19. H. Diamond, J. J. Hines, R. K. Sjoblom, R. F. Barnes, D. N. Metta, J. L. Lerner, and P. R. Fields, *Fission Cross-sections for ^{243}Pu , ^{250}Bk , ^{247}Cm , ^{254m}Es and ^{254}Es* , J. Inorg. and Nucl. Chem. 30, 2553-2559 (1968).
20. B. C. Diven, H. C. Martin, R. F. Taschek and J. Terrell, *Multiplicities of Fission Neutrons*, Phys. Rev. 101, 1012-1015 (1956).
21. B. C. Diven and J. C. Hopkins, *Numbers of Prompt Neutrons per Fission for ^{233}U , ^{235}U , ^{239}Pu and ^{252}Cf* , Proc. Phys. of Fast and Intermediate Reactors, Vol. I, IAEA (1961), pp. 149-154.
22. F. L. Fillmore, *Recommended Values for the Number of Neutrons per Fission*, J. Nucl. Energy 22, 79-97 (1968) [A survey and least-squares averaging].
23. S. C. Fultz, J. T. Caldwell, B. L. Berman, R. L. Bramblett, M. A. Kelly, H. D. Wilson, M. S. Coops, R. W. Lougheed, J. E. Evans, and R. W. Hoff, *Measurement of the Average Neutron Yield per Fission for ^{242m}Am* , Phys. Rev. 152, 1046-1049 (1966).
24. L. D. Gordeeva and G. N. Smirenkin, *An Empirical Formula for the Average Number of Fission Neutrons*, Sovt. J. Atomic Energy 14, 562-566 (1963); translation from Atomnaya Energiia 14, 530-534 (1963).
25. J. A. Grundl, *A Study of Fission-neutron Spectra with High-energy Activation Detectors, Part II: Fission Spectra*, Nucl. Sci. Eng. 31, 191-206 (1968).
26. T. R. Herold, *Energy Spectra of Neutrons and Gamma Rays from Spontaneous Fission of ^{244}Cm* , DP-949 (July 1965).
27. D. A. Hicks, J. Ise, Jr., and R. V. Pyle, *Spontaneous-Fission Neutrons of ^{252}Cf and ^{244}Cm* , Phys. Rev. 98, 1521-1523 (1955).
28. D. A. Hicks, J. Ise, Jr., and R. V. Pyle, *Probabilities of Prompt-Neutron Emission from Spontaneous Fission*, Phys. Rev. 101, 1016-1020 (1956).
29. G. H. Higgins, W. W. T. Crane, and S. R. Gunn, *Average Number of Neutrons per Spontaneous Fission of ^{244}Cm* , Phys. Rev. 99, 183 (1955).
30. J. C. Hopkins and B. C. Diven, *Prompt Neutrons from Fission*, Nucl. Phys. 48, 433-442 (1963).
31. W. F. Hornyak, *Fast Neutron Detector*, Rev. Sci. Instrum. 23, 264-267 (1952).
32. E. K. Hyde, *The Nuclear Properties* of the Heavy Elements*, Vol. III, *Fission Phenomena*, Prentice-Hall, New Jersey (1964), Ch. 3.
33. E. K. Hyde, *ibid.*, Ch. 7.

34. E. K. Hyde, *ibid.*, Ch. 8.
35. A. H. Jaffey, C. T. Hibdon, and R. Sjolblom, *Thermal Neutron ν for ^{241}Pu* , J. Nucl. Energy 11A, 21-30 (1959).
36. A. H. Jaffey and J. L. Lerner, *A Note on Error Estimation When a Calibration Curve Is Used*, ANL-7584 (July 1969).
37. U. I. Kalashnikova, V. I. Lebedev, L. A. Mikaelyan, P. E. Spivak, and V. P. Zakharova, "Relative Measurements of the Average Number of Neutrons Emitted in the Thermal Fission of ^{233}U , ^{235}U , ^{239}Pu and ^{241}Pu ," *Conf. Acad. Sci. USSR on the Peaceful Uses of Atomic Energy*, Session on Phys.-Math. Sci., Moscow (1956), p. 123.
38. V. P. Kovalev, V. N. Andreev, M. N. Nikolaev, and A. G. Guseinov, *Comparison of Neutron Spectra in the Fission of ^{233}U , ^{235}U , and ^{239}Pu* , Soviet Phys. JETP(6) 33, 825-826 (1958).
39. B. D. Kuzminov and G. N. Smirenkin, *Systematics of the Average Number ν of Prompt Fission Neutrons*, Sovt. Phys. JETP 7, 346-347 (1958). Translation from JETP (USSR) 34, 503-504 (1958).
40. V. I. Lebedev and V. I. Kalashnikova, *Mean Number of Neutrons Emitted in Fission of ^{241}Am by Thermal Neutrons*, Atomnaya Energiia 5, 176-177 (1958); translation in J. Nucl. Energy, Reactor Sci. 10, 90 (1959) and Soviet J. Atom. Energy 5, 1019-1020 (1958).
41. C. M. Lederer, J. M. Hollander, and I. Perlman, *Table of Isotopes*, 6th ed., John Wiley & Sons, Inc., New York (1967).
42. H. D. Lemmel and C. H. Westcott, *Fission and Absorption g -factors of ^{241}Pu* , J. Nucl. Energy 21, 417-424 (1967).
43. D. S. Mather, P. Fieldhouse, and A. Moat, *Average Number of Prompt Neutrons from ^{235}U Fission Induced by Neutrons from Thermal to 8 MeV*, Phys. Rev. 133B, 1403-1420 (1964).
44. J. W. Meadows and J. F. Whalen, *Energy Dependence of Prompt ν for Neutron-induced Fission of ^{235}U* , Phys. Rev. 126, 197-201 (1962).
45. J. W. Meadows and J. F. Whalen, *Energy Dependence of ν_p for Neutron-induced Fission of ^{235}U below 1.0 MeV*, J. Nucl. Energy 21, 157-169 (1967).
46. J. W. Meadows, *^{252}Cf Fission Neutron Spectrum from 0.003 to 15.0 MeV*, Phys. Rev. 157, 1076-1082 (1967).
47. A. Moat, D. S. Mather and M. H. McTaggart, *Some Experimental Determinations of the Number of Prompt Neutrons from Fission*, J. Nucl. Energy (Reactor Sci. and Technol.), Parts A/B, 15, 102-112 (1961).
48. F. L. Oetting and S. R. Gunn, *A Calorimetric Determination of the Specific Power and Half-life of Americium-241*, J. Inorg. Nucl. Chem. 29, 2659-2664 (1967).
49. K. G. Porges and A. DeVolpi, *Absolute Determination of Fission Fragment Emission Rates with Prompt Neutron-Fission Coincidence Method*, Proc. Symp. on Standardization of Radionuclides, IAEA, Vienna (1967), pp. 693-703.

- 50a. A. Prince, *Estimated Fission Properties of Transradium Isotopes*, 2nd Conf. Neutron Cross-Sections and Technology, Washington, D.C. (March 1968).
- 50b. A. Prince, private communication (1969).
51. J. E. Sanders, *A Comparison of the Average Number of Neutrons Emitted in Fission of Some Uranium and Plutonium Isotopes*, J. Nucl. Energy 2, 247-254 (1956).
52. K. Skarsvåg and K. Bergheim, *Energy and Angular Distributions of Prompt Neutrons from Slow Neutron Fission of ^{235}U* , Nucl. Phys. 45, 72-97 (1963).
53. A. B. Smith, P. R. Fields, and J. H. Roberts, *Spontaneous Fission Neutron Spectrum of ^{252}Cf* , Phys. Rev. 108, 411-413 (1957).
54. A. B. Smith, P. R. Fields, R. K. Sjöblom, and J. H. Roberts, *Precise Determination of the ^{233}U Fission Neutron Spectrum*, Phys. Rev. 114, 1351-1353 (1959).
55. J. R. Stehn, M. D. Goldberg, R. Wiener-Chasman, S. F. Mughabghab, B. A. Magurne, and V. M. May, *Neutron Cross-Sections, Vol. III, Z = 88 to 98*, BNL-325, 2nd ed., Suppl. No. 2 (Feb 1965).
56. J. Terrell, *Distribution of Fission Neutron Numbers*, Phys. Rev. 108, 783-789 (1957).
57. J. Terrell, *Fission Neutron Spectra and Nuclear Temperatures*, Phys. Rev. 113, 527-541 (1959).
58. J. Terrell, *Neutron Yields from Individual Fission Fragments*, Phys. Rev. 127, 880-904 (1962).
59. J. Terrell, *Prompt Neutrons from Fission*, Proc. Symp. on Phys. and Chem. of Fission, IAEA, Vienna (1965), pp. 3-24.
60. C. H. Westcott, K. Ekberg, G. C. Hanna, N. J. Pattenden, S. Sanatini, and P. M. Attree, *A Survey of Values of the 2200 m/s Constants for Four Fissile Nuclides*, Atomic Energy Review 3, 1-62 (1965).
61. C. H. Westcott and G. C. Hanna, private communication (1969).

ARGONNE NATIONAL LAB WEST



3 4444 00008228 9

8

